Expression profiling analysis of the CD5+ diffuse large B-cell lymphoma subgroup: Development of a CD5 signature

Miyuki Suguro,[1,2,3] Hiroyuki Tagawa,[1] Yoshitoyo Kagami,[4] Masataka Okamoto,[5] Koichi Ohshima,[6] Hiroshi Shiku,[3] Yasuo Morishima,[4] Shigeo Nakamura[7] and Masao Seto[1,8]

[1]Division of Molecular Medicine, Aichi Cancer Center Research Institute, Nagoya, Aichi 464-8681; [2]Japan Biological Informatics Consortium, Tokyo 135-0064; [3]Second Department of Internal Medicine, Mie University School of Medicine, Tsu, Mie 514-8507; [4]Division of Hematology and Cell Therapy, Aichi Cancer Center Hospital, Nagoya, Aichi 464-8681; [5]Department of Internal Medicine, Fujita Health University School of Medicine, Toyoake, Aichi 470-1192; [6]First Department of Pathology, Fukuoka University School of Medicine, Fukuoka 814-0180; [7]Pathology/Clinical Laboratories, Nagoya University Hospital, Nagoya, Aichi 466-8560, Japan

(Received March 15, 2006/Revised May 17, 2006/Accepted May 18, 2006/Online publication July 17, 2006)

Diffuse large B-cell lymphoma (DLBCL) accounts for 30% of non-Hodgkin's lymphomas and is known to comprise heterogeneous groups. We previously reported that CD5+ DLBCL is a clinically distinct subgroup of these tumors that is associated with poor prognosis. In our current study, we have used gene expression profiling technology in an attempt to identify new markers and to further characterize the biological features of CD5+ DLBCL. Candidate genes, which showed the greatest difference in expression between 22 CD5+ and 26 CD5- DLBCL cases, were selected from our screening and subjected to clustering analysis. This resulted in identification of a specific mRNA profile (a CD5 signature) for CD5+ DLBCL. The CD5 signature included downregulated extracellular matrix genes such as *POSTN, SPARC, COL1A1, COL3A1, CTSK, MMP9* and *LAMB3*, and comprised upregulated genes including *TRPM4*. We tested this CD5 signature for its potential use as a relevant marker for CD5+ DLBCL and found that it did indeed recognize this subgroup. The tumors identified by the CD5 signature contained most of the CD5+ DLBCL cases and some CD5- DLBCL cases. Moreover, the subgroup of cases with this CD5 signature showed a poorer prognosis. The subsequent application of the CD5 signature to the analysis of an independent series of DLBCL microarray data resulted in identification of a subgroup of DLBCL cases with a similar clinical outcome, further suggesting that the CD5 signature can be used as a clinically relevant marker of this disease. (*Cancer Sci* 2006; 97: 868–874)

Diffuse large B-cell lymphoma (DLBCL) is the most common form of non-Hodgkin's lymphoma.[1] Because it is known to include pathophysiologically and clinically heterogeneous groups, the proper identification of well-defined DLBCL subgroups has become an urgent requirement for clinicians. We previously reported that CD5+ DLBCL is a clinically distinct subgroup of DLBCL, accounting for 5–10% of all DLBCL.[2,3] Moreover, this subgroup of cases is characterized by more aggressive clinical features and poorer prognosis, compared with CD5- DLBCL.[3] Genomic aberrations that are characteristic of CD5+ DLBCL have also been identified.[4–6] CD5 positivity is essential for the detection of CD5+ DLBCL cases but is also a marker of mantle cell lymphoma (MCL), and indeed some instances of CD5+ DLBCL possess similar histological features to MCL. For such cases, the use of other markers such as cyclin D1 has become important,[1] and this indicates that the detection of CD5 alone is not sufficient to define the entire spectrum of CD5+ DLBCL tumors. Hence, CD5 can serve as an effective marker when it is used in combination with other biological indicators but it is clear that more effective markers for CD5+ DLBCL will need to be identified.

Expression profiling of mRNA has been used previously as a marker for subgroups of DLBCL.[7–10] Activated B-cell-like (ABC) and germinal-center B-cell-like (GCB) DLBCL are examples of subgroups of DLBCL that have been identified in this way.[7,8] It is thus possible that the use of expression profiling can yield novel and effective markers for defining subgroups of DLBCL, in conjunction with established markers such as CD5. With these findings in mind, we compared the expression profiles of 22 cases of CD5+ and 26 cases of CD5- DLBCL in the present study to identify better markers that may provide new insights into our understanding of the pathobiology of CD5+ DLBCL.

Materials and Methods

Patients and samples

The lymph node samples and clinical data used in our present analyses were obtained through an Institutional Review Board approved protocol from 22 patients with CD5+ DLBCL, and a further 26 individuals with CD5- DLBCL. Within these subject groups, 74% of the CD5+ DLBCL cases (14/17) and 29% of the CD5- DLBCL cases (7/24) were associated with extranodal sites (at least one site). None of these patients had a previous history of lymphoma and all 48 individuals received adequate treatment with cyclophosphamide, adriamycin, vincristine and predonine (CHOP)-like regimens. The median follow-up time was 2.4 years and the 5-year overall survival rate of the DLBCL patients was 40%. Each of the 22 CD5+ DLBCL cases was

[8]To whom correspondence should be addressed. E-mail: mseto@aichi-cc.jp

doi: 10.1111/j.1349-7006.2006.00267.x
© 2006 Japanese Cancer Association

diagnosed for CD5 positivity by immunohistology and four of these cases were confirmed by fluorescence-activated cell sorter (FACS) analysis. All of the 26 $CD5^-$ DLBCL cases were diagnosed for CD5 negativity also by immunohistology and 23 of these were confirmed by FACS analysis. Either Leu1 (Becton Dickinson, Mountain View, CA, USA) or 4C7 (Novocastra, Newcastle, UK) was used as the monoclonal antibody for detection of CD5 antigen. The lymphomas were judged to be CD5 positive when more than 20% of the tumor cells showed positive staining.[3] Classical cytogenetics was used to confirm a negative t(11;14) in each case to exclude the diagnosis of a large cell variant of mantle cell lymphoma.

Microarray procedures

Total RNA extracts were isolated from each specimen by cesium chloride centrifugation, as described previously.[11] An oligonucleotide array, custom-made for the Cancer Institute of the Japanese Foundation for Cancer Research and on which 21 619 genes had been spotted, was used for analysis according to the manufacturer's protocol (Agilent Technologies, Palo Alto, CA, USA). The probe consisted of a mixture of an experimental Cy5-labeled cRNA and control Cy3-labeled cRNA, with the latter prepared from a pool of total RNA from 10 hyperplastic lymph node samples. Non-flagged array elements with a fluorescent intensity greater than 300 (one standard deviation below the mean of all fluorescent data) were considered well measured. Ratios of the fluorescence of the experimental Cy5-labeled samples to that of the Cy3-labeled controls were then log transformed (base 2).

Clustering analyses of microarray data

Genes that showed the greatest average difference in expression between 22 cases of $CD5^+$ and 26 cases of $CD5^-$ DLBCL after log transformation were selected from the screening. A hierarchical clustering algorithm was then applied to the DLBCL cases, according to the expression level of these genes, with the aid of Cluster and TreeView programs (http://rana.lbl.gov/EisenSoftware.htm).[12] The classification of either ABC or GCB DLBCL was based on the analysis of 100 genes identified in a previous study.[8] Our array slides contained 67 of these genes, which we used in a simple clustering method. Log-transformed ratios were centered by subtracting the median observed value of each of the genes for clustering analysis.[8]

Analysis of the published microarray data

The DLBCL gene expression profile data generated by the Cancer Genomics group were obtained from the supplemental data listed in at http://www.broad.mit.edu/cancer/pub/dlbcl.[10] None of the 176 DLBCL cases listed here had a previous history of lymphoma. The array fluorescence of these genes was log-transformed and centered by subtracting the median observed value of each of the genes for clustering analysis.

Results

Identification of CD5 signature genes for the $CD5^+$ DLBCL subgroup

Genes showing differential expression between 22 $CD5^+$ and 26 $CD5^-$ DLBCL were identified and 24 of these candidates showed an average expression difference of more than 2.5-fold between these tumor subgroups (Fig. 1a). These genes were therefore selected for clustering analysis and are referred to as CD5 signature genes. A further 70 genes showing a difference of more than 2-fold were also subjected to the same analysis.

Clustering analysis of CD5 signature genes in $CD5^+$-type and $CD5^-$-type DLBCL

Hierarchical clustering analysis with each of the identified 24 CD5 signature genes, applied to all 48 DLBCL cases, is shown in Fig. 1b. A further series of analyses using the 70 genes produced almost identical results (data not shown). It was noted that many of the genes that were found to be downregulated in $CD5^+$ DLBCL, such as *POSTN*, *SPARC*, *COL1A1*, *COL3A1*, *CTSK*, *MMP9* and *LAMB3*, are associated with the extracellular matrix (Fig. 1b). *UCHL1* and *CR2* were also found to be downregulated in $CD5^+$ DLBCL tumors and are known to be expressed in T cells, macrophages and follicular dendritic cells, which are subsets of cells that function during the immune response (Fig. 1b).

Our clustering analysis further enabled us to classify the DLBCL cases under study into two groups, one comprising 20 $CD5^+$ and 11 $CD5^-$ DLBCL cases, and the other consisting of 14 $CD5^-$ and two $CD5^+$ DLBCL samples (Fig. 1b). This indicated that the CD5 signature genes could potentially serve as markers for subgroups that are related to $CD5^+$ DLBCL. All except two cases of $CD5^+$ DLBCL could be included in the first of these two groups, which we designated as $CD5^+$-type DLBCL, in order to distinguish it from $CD5^+$ DLBCL (Table 1). The second group is referred to as $CD5^-$-type DLBCL (Table 1). One $CD5^-$ DLBCL case could not be assigned to either of these subgroups. The clinical features of $CD5^+$-type and $CD5^-$-type DLBCL are shown in Table 2. Patients with $CD5^+$-type DLBCL showed a more advanced tumor stage at diagnosis, compared with the $CD5^-$-type DLBCL cases (stage III/IV: 90% and 50%, respectively; $P = 0.0062$), and also displayed a higher international prognostic index[13] (IPI score 3–5: 66% and 27%, respectively; $P = 0.0398$). In addition, the overall survival of patients with $CD5^+$-type DLBCL after treatment with CHOP-like regimens was significantly poorer than patients with $CD5^-$-type DLBCL (Fig. 1c; $P = 0.0006$).

In the $CD5^+$-type DLBCL group, we assigned 11 $CD5^-$ DLBCL cases (Table 1), and these were further examined to explore whether in fact any similarities to $CD5^+$ DLBCL existed. Both groups showed similar clinical features except for performance status (Table 3) and no significant differences in survival were observed between the two ($P = 0.31$, log-rank test; data not shown). However, the $CD5^-$ DLBCL cases in the $CD5^+$-type DLBCL group did show a significantly poorer prognosis than their $CD5^-$ DLBCL counterparts in the $CD5^-$-type DLBCL group ($P = 0.0333$; data not shown), indicating that these 11 $CD5^-$ DLBCL cases had some clinical features that could be regarded as similar to $CD5^+$ DLBCL.

Incidence of ABC and GCB DLBCL among the 48 DLBCL subject cases

Clustering analysis using 67 of the 100 established ABC and GCB markers[8] was applied to our current 48 DLBCL cases, and it was found that these cases could be classified as either

© 2006 Japanese Cancer Association

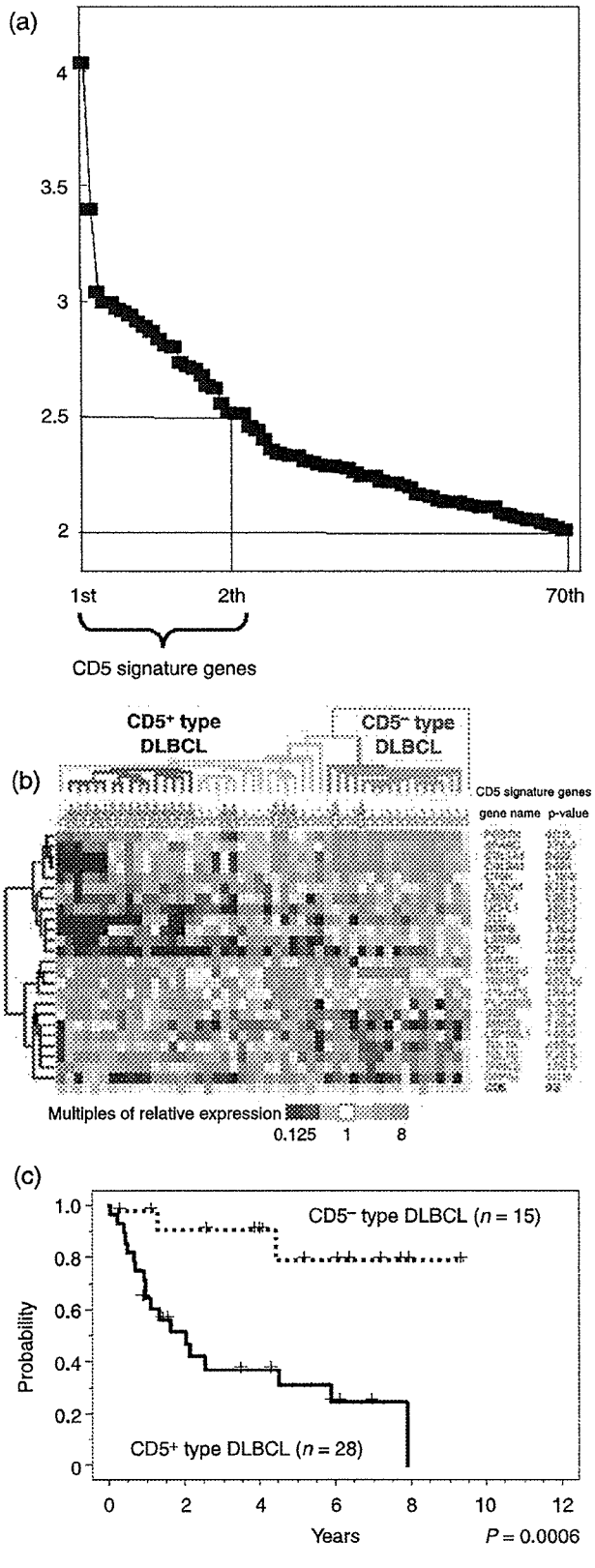

Table 1. Diffuse large B-cell lymphoma (DLBCL) subgroups defined by different markers

Surface marker	mRNA profiling marker	
	$CD5^+$-type DLBCL ($n = 31$)	$CD5^-$-type DLBCL ($n = 16$)
$CD5^+$ DLBCL ($n = 22$)	20	2
$CD5^-$ DLBCL ($n = 25$)	11	14
		$P = 0.0008^\dagger$

†*P*-values were calculated with Fisher's exact test.

ABC or GCB DLBCL (Fig. 2a). Kaplan–Meier analysis further revealed that the ABC DLBCL cases under analysis showed a significantly poorer prognosis, compared with the GCB DLBCL samples (Fig. 2b; $P = 0.0028$). This is in agreement with results reported previously.[7,8]

Application of the CD5 signature to published microarray data

In order to further test the validity of our CD5 signature, we applied it to published microarray data. Among the data from the Cancer Genomics group, comprising the expression level of 44 792 genes from 176 DLBCL cases, we were able to locate 22 (91%) of the 24 CD5 signature genes. Clustering analysis of these DLBCL cases, carried out with 22 of the CD5 signature genes, identified two subgroups of DLBCL, showing downregulation and upregulation of extracellular matrix genes, respectively (Fig. 3a). In addition, the mRNA profiles of these subgroups were similar to the profiles obtained from our current DLBCL cases, such that the first subgroup could be identified as $CD5^+$-type and the second subgroup as $CD5^-$-type. The $CD5^+$-type DLBCL cases again showed a

Fig. 1. CD5 signature genes define $CD5^+$-type and $CD5^-$-type diffuse large B-cell lymphoma (DLBCL). (a) Differences in the expression of CD5 signature genes. Genes showing the highest level of differential expression between 22 $CD5^+$ and 26 $CD5^-$ DLBCL cases are aligned, and multiples of the average differences in their expression levels are shown on the vertical axis. Twenty-four genes showing an average difference of more than 2.5-fold between the subgroups were designated as the CD5 signature genes. Seventy genes in total showed a difference of more than 2.0-fold. (b) Hierarchical clustering of 48 DLBCL cases via the expression levels of the 24 CD5 signature genes. Each row represents one gene. The dendrogram on the left shows the degree to which each gene is related to the others. Half of the CD5 signature genes in $CD5^+$ DLBCL showed low expression levels (upper portion of the figure, shown in blue), some of which were related to the extracellular matrix (*POSTN*, *SPARC*, *COL1A1*, *COL3A1*, *CTSK*, *MMP9* and *LAMB3*). The remaining CD5 signature genes in $CD5^+$ DLBCL showed high expression (lower portion of the figure, shown in red). The relative expression of *CD5* for each sample is indicated at the bottom of the figure, which also shows the *P*-values of these genes, determined using the Student's *t*-test. Each column represents one DLBCL case and the dendrogram on the top shows the degree to which each DLBCL is related to the other tumor samples in terms of gene expression. The DLBCL cases were divided into two subgroups: $CD5^+$-type (left) and $CD5^-$-type DLBCL (right). There was a cluster of 15 $CD5^+$ DLBCL cases at the core of the $CD5^+$-type DLBCL group (marked with dark blue lines). One $CD5^-$ DLBCL case, located in a row on the extreme right, belonged to neither of the subgroups. (c) Kaplan–Meier analysis of the $CD5^+$-type and the $CD5^-$-type DLBCL cases in this study. The $CD5^+$-type DLBCL patients showed a significantly poorer prognosis than their $CD5^-$-type DLBCL counterparts. The *P*-values for these subgroups were analyzed using the log-rank test.

doi: 10.1111/j.1349-7006.2006.00267.x
© 2006 Japanese Cancer Association

Table 2. Characteristics of patients with diffuse large B-cell lymphoma (DLBCL)

Characteristic	$CD5^+$-type DLBCL ($n = 31$)		$CD5^-$-type DLBCL ($n = 31$)		*P*-value†
	n	%	*n*	%	
IPI factor					
Age > 60 years	20	65	11	69	>0.99
Stage > 2	27	90	7	50	0.0062
LDH > normal	23	79	10	91	0.65
Performance status > 1	8	28	0	0	0.08
Extranodal site > 1	8	30	1	7	0.13
IPI score 3–5 (high)	19	66	3	27	0.0398

†*P*-values were calculated with Fisher's exact test. IPI, international prognostic index; LDH, lactate dehydrogenase.

Table 3. Characteristics of patients with $CD5^+$ diffuse large B-cell lymphoma (DLBCL) and $CD5^-$ cases in the $CD5^+$-type DLBCL subgroup

Characteristic	$CD5^+$ DLBCL ($n = 22$)		$CD5^-$ DLBCL cases in the DLBCL subgroup ($n = 22$)		*P*-value†
	n	%	*n*	%	
IPI factor					
Age > 60 years	13	59	8	73	0.70
Stage > 2	19	95	9	82	0.28
LDH > normal	17	85	7	70	0.37
Performance status > 1	8	40	0	0	0.0288
Extranodal site > 1	6	32	3	30	>0.99
IPI score 3–5 (high)	14	70	6	60	0.69

†*P*-values were calculated with Fisher's exact test. IPI, international prognostic index; LDH, lactate dehydrogenase.

trend toward a poorer prognosis than their $CD5^-$-type counterparts, although this difference was not statistically significant ($P = 0.0762$; Fig. 3b).

We investigated the relationship between $CD5^+$-type and $CD5^-$-type DLBCL, and also between ABC and GCB DLBCL. The 176 DLBCL cases were divided into 34 cases of ABC DLBCL, 85 cases of GCB DLBCL and 57 cases of classless leftovers on the basis of published data.[10,14] These ABC and GCB DLBCL cases could be divided into $CD5^+$-type and $CD5^-$-type DLBCL groups, so that the DLBCL cases could be classified into four subgroups by combining these two different modes of expression profiling. In the ABC DLBCL group, the $CD5^+$-type cases showed a poorer prognosis than the $CD5^-$-type cases (Fig. 4a; $P = 0.0397$). However, in the GCB DLBCL group, there was no significant difference in survival outcome between the $CD5^+$-type and the $CD5^-$-type cases (Fig. 4b; $P = 0.5073$). Thus, the clinical outcome for the $CD5^+$-type cases in the ABC DLBCL group was poorer than the outcomes in the other three subgroups.

We also attempted to apply the CD5 signature to other published microarray data. However, as only eight (33%) of the 24 CD5 signature genes could be found among the Lymphochip microarray data,[8] we considered that the results of any analysis using so few genes would not be meaningful.

Discussion

In a Japanese study, $CD5^+$ DLBCL was identified as a known subgroup of DLBCL that is associated with poor prognosis.[3] Furthermore, $CD5^+$ malignancies in Asian countries are different from those in Western countries, as evidenced by the incidence of chronic lymphocytic leukemia (CLL), which is the most frequent leukemia in Europe and the USA, but occurs at one-fifth of this rate in Japan.[1,15,16] In this regard, clinicians in Asian countries are in a better situation to investigate $CD5^+$ DLBCL due to a lower level of noise that would be caused by high incidence of CLL and CLL-related malignancies. In our current study, we attempted to elucidate novel markers and further characterize the biological features of $CD5^+$ DLBCL by means of expression profiling. Differentially expressed genes between $CD5^+$ and $CD5^-$ DLBCL samples were selected and subjected to clustering analyses, resulting in the identification of a specific mRNA profile of $CD5^+$ DLBCL, which we refer to as a CD5 signature.

The CD5 signature shows a characteristic profile featuring downregulated genes that are associated with the extracellular matrix. This profile was also found in the DLBCL samples from independent array data. The lack of an extracellular matrix may well be partially responsible for the aggressive clinical features that are characteristic of $CD5^+$ DLBCL. Our CD5 signature was compared with some reported gene sets that are concerned with the DLBCL subgroups. (1) Gascoyne *et al.* have reported 10 genes to be differentially expressed in $CD5^+$ and $CD5^-$ DLBCL.[17] *MMP9* is one of these genes and was in fact included in our CD5 signature gene set. (2) Kobayashi *et al.* have previously described an mRNA profile for $CD5^+$ DLBCL,[18] but our current findings are somewhat discordant with these previous data. The study of Kobayashi *et al.* reported

© 2006 Japanese Cancer Association

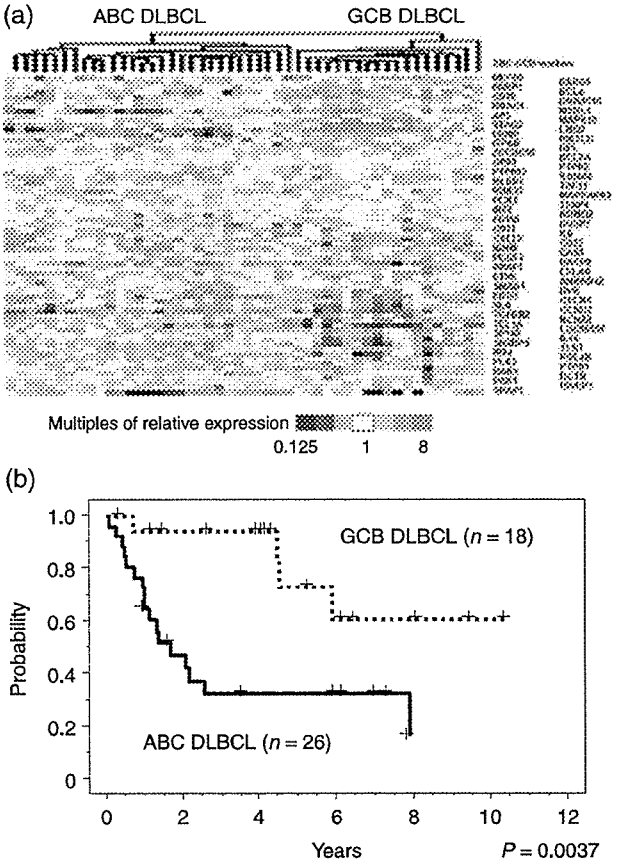

Fig. 2. Designation of activated B-cell-like (ABC) and germinal-center B-cell-like (GCB) diffuse large B-cell lymphoma (DLBCL) subtypes among the 48 DLBCL cases in this study. (a) Hierarchical clustering of the 48 DLBCL subject cases based on the expression levels of 67 known ABC and GCB marker genes that are also common to our dataset.[8] Our DLBCL samples were classified as ABC (left) and GCB (right) DLBCL in terms of the specific mRNA profiles of these marker genes. (b) Kaplan–Meier analysis of the ABC and GCB DLBCL samples among the current 48 DLBCL cases. This survival analysis showed significant differences between these subgroups.

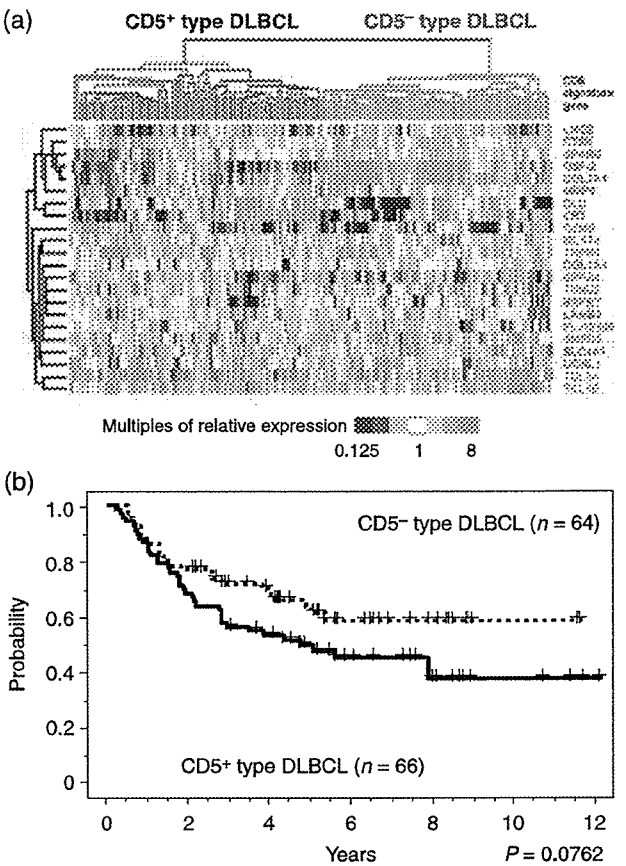

Fig. 3. Characterization of CD5⁺-type and CD5⁻-type diffuse large B-cell lymphoma (DLBCL) with existing published microarray data. (a) Clustering analysis of DLBCL samples from the Cancer Genomics group in terms of the expression levels of 22 of the CD5 signature genes. The DLBCL samples from published microarray data were classified as CD5⁺-type (left) and CD5⁻-type (right) DLBCL. The CD5⁺-type DLBCL was again characterized by downregulation of the genes that are related to the extracellular matrix, but there were some exceptions. The genes that showed a low expression level in our CD5⁺-type DLBCL cases (Fig. 1b) are indicated in blue and those with high expression (Fig. 1b) are shown in red. (b) Kaplan–Meier analysis of the Cancer Genomics group DLBCL patients that were subgrouped by means of the CD5 signature. The CD5⁺-type DLBCL patients again showed poorer prognosis than the CD5⁻-type DLBCL patients, although this difference was found not to be statistically significant. The *P*-values for these subgroups were analyzed with the log-rank test.

ITGB1 as one of the strong classifier genes showing high expression in CD5⁺ DLBCL, whereas our present analysis shows its expression in CD5⁺ DLBCL to be 1.28 times lower on average, compared with CD5⁻ DLBCL. The classifier gene *CD36* was also reported by Kobayashi *et al.* to show high expression levels in CD5⁺ DLBCL, but was found to be only 1.29 times higher in our present analysis. Significantly, none of the CD5 signature genes that we identified overlap with these previously characterized classifiers. These differences may be partly due to the fact that the study of Kobayashi *et al.* incorporated a 2400 spotted array, whereas we have used a 21 619 gene array. (3) The lymph-node signature is a profile of DLBCL reportedly related to clinical outcome and includes many extracellular matrix-associated genes.[8] Of these 375 lymph-node signature genes, 124 were included in our present data set and a further eight of our 24 CD5 signature genes can be found in their data set.[8] However, only three of these CD5 signature genes overlap, whereas the remaining five differ from the lymph-node signature genes, suggesting that our CD5 signature is likely to be different from the lymph-node signature. (4) We previously reported that ABC DLBCL was closely related to CD5⁺ DLBCL,[6] but none of the ABC and GCB markers[7] overlap with the CD5 signature genes. However, *IRF4*, which is one of the markers that shows high expression in ABC DLBCL, was found in our current analysis to be expressed at a level that was on average 1.56 times higher in CD5⁺ DLBCL than in CD5⁻ DLBCL. Other markers that have low expression in ABC DLBCL include

doi: 10.1111/j.1349-7006.2006.00267.x
© 2006 Japanese Cancer Association

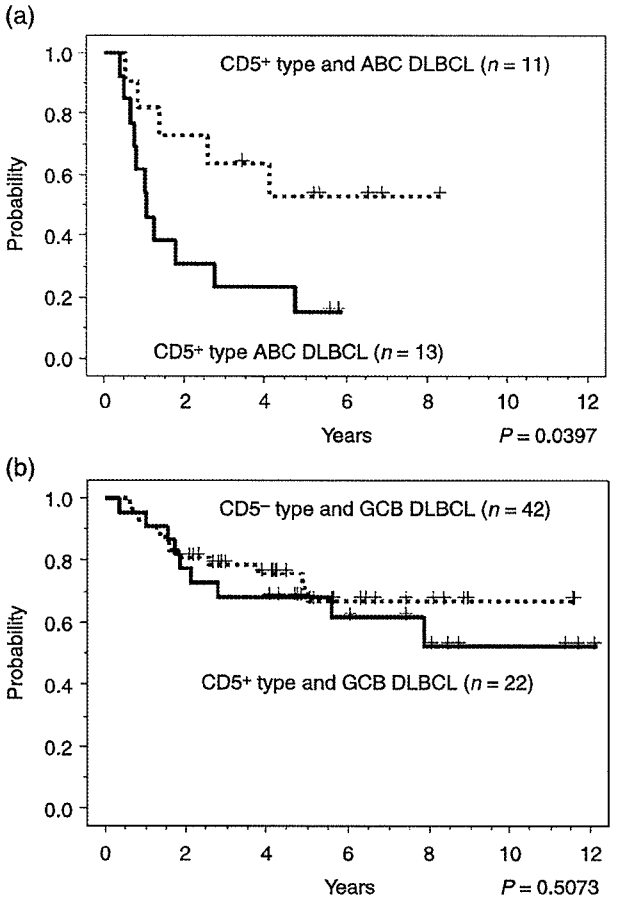

Fig. 4. Comparison of the CD5⁺-type and the CD5⁻-type diffuse large B-cell lymphoma (DLBCL) in combination with activated B-cell-like (ABC) and germinal-center B-cell-like (GCB) DLBCL. Kaplan–Meier analysis of (a) ABC DLBCL and (b) GCB DLBCL patients from the Cancer Genomics group subgrouped by means of the CD5 signature. The clinical outcomes were poorest for ABC patients with CD5⁺-type DLBCL. In contrast, there was no significant difference in survival outcome between the CD5⁺-type and the CD5⁻-type GCB subgroups. The *P*-values for these subgroups were analyzed with the log-rank test.

CD10 and *BCL6*, expressed 1.39 times and 1.88 times lower, respectively, in CD5⁺ DLBCL, and this is in agreement with results reported previously.[6] (5) Array comparative genomic hybridization (CGH) analyses have previously uncovered some genomic imbalances that characterize CD5⁺ DLBCL,[5,6] one of which is a loss of 9p21. This is consistent with our present mRNA profile analysis, which shows that the expression of *CDKN2A*, located on 9p21, is on average 1.5 times lower in CD5⁺ DLBCL, compared with CD5⁻ DLBCL. However, we did not include this gene in the CD5 signature because its differential expression was lower than the 2.5-fold cut-off threshold. This threshold for inclusion in the CD5 signature is probably one of the reasons why none of the CD5 signature genes is located on chromosomal loci that have been shown to be lost or gained in lymphoma.

Although the CD5 signature genes are statistically representative of CD5⁺ DLBCL, there were some CD5⁻ DLBCL cases found to express the CD5 signature. Eleven of 26 CD5⁻ DLBCL cases expressed the CD5 signature, according to our microarray data, and although only 5–10% of the published cases were expected to be CD5⁺ DLBCL,[3] 50% of all DLBCL cases from the Cancer Genomics group were found to express the CD5 signature. The incidence of CD5⁻ DLBCL cases expressing the CD5 signature can be partly explained by the results of the clustering analysis of our current cases (Fig. 1b). The CD5⁺-type DLBCL group that we identified is composed of two parts: a central cluster consisting of only CD5⁺ DLBCL cases and the rest comprising mainly CD5⁻ DLBCL patients. This indicates that the CD5 signature provides a rough identification of CD5⁻ DLBCL with expression profiles that are similar to those of CD5⁺ DLBCL, and that these cases may in fact resemble CD5⁺ DLBCL. Indeed, these same CD5⁻ DLBCL cases did show clinical features that resemble CD5⁺ DLBCL. We speculate that CD5⁻ DLBCL cases that show clinical features similar to CD5⁺ DLBCL will become evident also in independent array data sets.

We utilized CD5 mRNA expression levels to determine which samples could be assigned to the CD5⁺ DLBCL subgroup among the available DLBCL cases of the Cancer Genomics group. However, this turned out to be ineffective because the CD5 expression levels evaluated by microarray did not correlate with the results obtained by immunostaining or FACS analysis. This discrepancy was most likely caused by background cells such as T cells that express CD5 more strongly than CD5⁺ DLBCL. However, when the CD5 signature was applied to independent data sets, it was found to be a useful tool that could be used to assign CD5⁺ DLBCL cases.

The CD5⁺-type DLBCL tumors showed a significantly poorer clinical outcome than the CD5⁻-type DLBCL in our present analysis. The significance of the differences in survival outcome between CD5⁺-type and CD5⁻-type DLBCL was further examined by analysis of the independent data set from the Cancer Genomics group and the *P*-value for this set was calculated as 0.0762, whereas that for our current study was 0.0037. Although the independent data set did not show significance, there was a measurable trend toward a poor prognosis, which should be noted. Interestingly, however, the CD5⁺-type DLBCL of the ABC type showed the worst prognosis, whereas the CD5⁻-type DLBCL of the ABC type showed a better prognosis that was almost equivalent to the GCB DLBCL cases. The two types of DLBCL of the GCB type, however, showed no significant difference in clinical outcome. We contend therefore that the CD5 signature could serve as an effective future marker of DLBCL when used in combination with ABC/GCB profiling subtypes. Hence, both ABC/GCB and the CD5 signatures are likely to be effective in identifying the DLBCL subtype with the poorest prognosis and to thus help determine the most appropriate treatment for DLBCL patients.

Acknowledgments

We wish to express our appreciation to Miss H. Suzuki and Miss Y. Kasugai for their outstanding technical assistance. We also thank Dr Ryuzo Ohno, the president of the Aichi Cancer Center, for his support. This work was supported in part by Grants-in-Aid from the Japan New Energy and

© 2006 Japanese Cancer Association

Industrial Technology Development Organization (NEDO) and the Ministry of Economy, Trade and Industry (METI), the Ministry of Health, Labor and Welfare, the Ministry of Education, Culture, Sports Science and Technology, the Japan Society for the Promotion of Science, and the Foundation of Promotion of Cancer Research. Additional support was also obtained via a Research Grant from the Princess Takamatsu Cancer Research Fund (03-23503).

References

1 Gatter KC, Warnke RA. Diffuse large B-cell lymphoma. In: Jaffe ES, Harris NL, Stein H, Vardiman JW, eds. *World Health Classification of Tumors. Pathology and Genetics of Tumours of Haematopoietic and Lymphoid Tissues*. Washington: IARC Press, 2001; 171–4.
2 Harada S, Suzuki R, Uehira K *et al.* Molecular and immunological dissection of diffuse large B cell lymphoma: $CD5^+$, and CD5 with $CD10^+$ groups may constitute clinically relevant subtypes. *Leukemia* 1999; **13**: 1441–7.
3 Yamaguchi M, Seto M, Okamoto M *et al.* De novo $CD5^+$ diffuse large B-cell lymphoma: a clinicopathologic study of 109 patients. *Blood* 2002; **99**: 815–21.
4 Karnan S, Tagawa H, Suzuki R *et al.* Analysis of chromosomal imbalances in *de novo* CD5-positive diffuse large-B-cell lymphoma detected by comparative genomic hybridization. *Genes Chromosomes Cancer* 2004; **39**: 77–81.
5 Tagawa H, Tsuzuki S, Suzuki R *et al.* Genome-wide array-based comparative genomic hybridization of diffuse large B-cell lymphoma: Comparison between CD5-positive and CD5-negative cases. *Cancer Res* 2004; **64**: 5948–55.
6 Tagawa H, Suguro M, Tsuzuki S *et al.* Comparison of genome profiles for identification of distinct subgroups of diffuse large B-cell lymphoma. *Blood* 2005; **106**: 1770–7.
7 Alizadeh AA, Eisen MB, Davis RE *et al.* Distinct types of diffuse large B-cell lymphoma identified by gene expression profiling. *Nature* 2000; **403**: 503–11.
8 Rosenwald A, Wright G, Chan WC *et al.* The use of molecular profiling to predict survival after chemotherapy for diffuse large-B-cell lymphoma. *N Engl J Med* 2002; **346**: 1937–47.
9 Shipp MA, Ross KN, Tamayo P *et al.* Diffuse large B-cell lymphoma outcome prediction by gene-expression profiling and supervised machine learning. *Nat Med* 2002; **8**: 68–74.
10 Monti S, Savage KJ, Kutok JL *et al.* Molecular profiling of diffuse large B-cell lymphoma identifies robust subtypes including one characterized by host inflammatory response. *Blood* 2005; **105**: 1851–61.
11 Seto M, Yamamoto K, Iida S *et al.* Gene rearrangement and over-expression of PRAD1 in lymphoid malignancy with +(11;14)(q13; q32) translocation. *Oncogene* 1992; **7**: 1401–6.
12 Eisen MB, Spellman PT, Brown PO, Botstein D. Cluster analysis and display of genome-wide expression patterns. *Proc Natl Acad Sci USA* 1998; **95**: 14863–8.
13 The International Non-Hodgkin's Lymphoma Prognostic Factors Project. A predictive model for aggressive non-Hodgkin's lymphoma. *N Engl J Med* 1993; **329**: 987–94.
14 Wright G, Tan B, Rosenwald A *et al.* A gene expression-based method to diagnose clinically distinct subgroups of diffuse large B cell lymphoma. *Proc Natl Acad Sci USA* 2003; **100**: 9991–6.
15 The World Health Organization classification of malignant lymphomas in Japan: Incidence of recently recognized entities. Lymphoma Study Group of Japanese Pathologists. *Pathol Int* 2000; **50**: 696–702.
16 Tamura K, Sawada H, Izumi Y *et al.* Chronic lymphocytic leukemia (CLL) is rare, but the proportion of T-CLL is high in Japan. *Eur J Haematol* 2001; **67**: 152–7.
17 Gascoyne RD, Dave S, Zettl A *et al.* Gene expression microarray analysis of *de novo* $CD5^+$ diffuse large B-cell lymphoma (LLMPP Study): a distinct entity? *Blood* 2003; **102**: 178a.
18 Kobayashi T, Yamaguchi M, Kim S *et al.* Microarray reveals differences in both tumors and vascular specific gene expression in *de novo* $CD5^+$ and $CD5^-$ diffuse large B-cell lymphomas. *Cancer Res* 2003; **63**: 60–6.

doi: 10.1111/j.1349-7006.2006.00267.x
© 2006 Japanese Cancer Association

Characterization of target genes at the 2p15–16 amplicon in diffuse large B-cell lymphoma

Noriko Fukuhara,[1,2] Hiroyuki Tagawa,[1] Yoshihiro Kameoka,[1] Yumiko Kasugai,[1] Sivasundaram Karnan,[1] Junichi Kameoka,[2] Takeshi Sasaki,[2] Yasuo Morishima,[3] Shigeo Nakamura[4] and Masao Seto[1,5]

[1]Division of Molecular Medicine, Aichi Cancer Center Research Institute, Nagoya 464-8681, [2]Department of Rheumatology and Hematology, Tohoku University School of Medicine, Sendai 980-8574, [3]Department of Hematology and Cell Therapy, Aichi Cancer Center Hospital, Nagoya 464-8681, [4]Pathology/Clinical Laboratories, Nagoya University Hospital, Nagoya 466-8550, Japan

(Received November 4, 2005/Revised January 26, 2006/Accepted February 20, 2006/Online publication May 11, 2006)

Amplification of 2p has been observed as a recurrent alteration in diffuse large B-cell lymphoma (DLBCL). Whereas two candidate oncogenes, *REL and BCL11A*, have been investigated as targets for 2p amplification, the question remains as to whether the true target gene in the amplicon is *REL*, *BCL11A* or both. We previously identified frequent genomic gains of chromosomal 2p in 25 out of 99 DLBCL cases by means of genome-wide array comparative genomic hybridization (CGH). All of these 25 cases included recurrent copy number gain at 2p15–16. In the study presented here, cases were analyzed in greater detail by means of contig bacterial artificial chromosome (BAC) array CGH for the 4.5-Mb region at 2p15–16, which contained 33 BAC clones. We confined the minimal common region to 500-kb in length, where only the candidate oncogene *REL*, and not *BCL11A*, is located. Real-time quantitative PCR was carried out to investigate the correlation between genomic gain and expression. It showed a significant correlation for both genes, indicating that these two genes are common targets for the 2p15–16 amplicon. However, given the fact that *REL* is more frequently amplified than *BCL11A*, the *REL* gene may play a more important role than *BCL11A* in the pathogenesis of DLBCL. (*Cancer Sci* 2006; 97: 499–504)

Diffuse large B cell lymphoma (DLBCL) is the most common type of malignant lymphoma, accounting for 30% of adult non-Hodgkin's lymphoma.[1] However, clinicopathological and genetic heterogeneities in this entity have suggested that further refinement of its subgroups is required.[2–5] Array-based comparative genomic hybridization (array-CGH) analysis is a powerful tool to identify genomic imbalances characteristic of distinct subgroups in DLBCL.[6,7] It has been useful not only for genome scanning of tumor cells but also for identification of novel oncogenes and suppressor genes.[8]

We previously used a genome-wide array-CGH to identify a gain of 2p15–16 in 25 out of 99 DLBCL cases.[7] Amplification at the 2p arm has been reported in B-cell lymphomas, such as DLBCL,[9–15] classical Hodgkin's lymphoma (cHL),[16,17] follicular lymphoma (FL)[18] and primary mediastinal B-cell lymphoma (PMBCL).[11,14,15] The two candidate genes, *REL* and *BCL11A*, have been mapped within this 2p15–16 amplicon. The *REL* proto-oncogene, which encodes a member of the NF-κB transcription factor family, has frequently been found amplified in B-cell lymphomas. *BCL11A*, which is located quite near *REL* on chromosome 2p15–16, is coamplified with *REL* in DLBCL and cHL.[12,15,16] In spite of numerous studies of this region, the question remains whether the target gene in the 2p15–16 amplification is *REL*, *BCL11A*, or both.

For the study presented here, we carried out a contig array-CGH using glass slides on which contiguously ordered bacterial artificial chromosome (BAC) clones were spotted throughout 4.5 Mb of the 2p15–16 genome to confine the minimal common region of amplification at 2p15–16 in DLBCL cases. Real-time quantitative–polymerase chain reaction (RQ-PCR) analysis was then used to further investigate the relationship between genomic amplification and expression.

Patients, Materials and Methods

Tumor samples

Tumor samples were obtained from 99 patients under a protocol approved by the International Review Board of the Aichi Cancer Center. Informed consent was obtained in accordance with the Declaration of Helsinki. All of the DNA and RNA samples were obtained from tumors at the time of diagnosis before the administration of any treatment. DNA was extracted with a standard phenol chloroform method from lymphoma specimens of the tumors. Normal DNA was prepared from peripheral-blood lymphocytes of healthy male donors. Total RNA was extracted using the standardized guanidium isothiocyanate and cecium chloride method from lymphoma specimens taken from the tumors. Data for genomic gains and losses at the chromosome 2 region of the 99 DLBCL have been reported previously.[7]

Genome-wide array-based CGH

DNA preparation, labeling, array fabrication and hybridization were carried out as described elsewhere.[6,8,19] Briefly, the array consisted of 2213 BAC and P-1-derived artificial chromosome (PAC) clones, covering the whole human genome with a resolution of 1.3 Mb, from library RP11, 13 for BAC clones and RP1, and 3, 4, 5 for PAC clones. Of the 2213 clones spotted on the glass slides, 188 were of chromosome 2, and of these 188 BAC/PAC clones, 75 were of the short arm of chromosome 2 (2p). These clones were obtained from the BAC/PAC Resource Center at the Children's Hospital Oakland Research Institute, Oakland,

[5]To whom correspondence should be addressed. E-mail: mseto@aichi-cc.jp

doi: 10.1111/j.1349-7006.2006.00209.x
© 2006 Japanese Cancer Association

CA, USA (http://bacpac.chori.org/). The thresholds for the $\log_2$ ratio of gains and losses were set at the $\log_2$ ratios of +0.2 and −0.2, respectively. High-level copy number gain (amplification) was defined as $\log_2$ ratio ≥ +1 and low-level copy number gain as $+0.2 \leq \log_2$ ratio $< +1.0$.[8]

Contig array-based CGH

Detailed analysis with contig array-CGH was carried out for cases with amplification ($n = 3$) and gain ($n = 4$, cases with available RNA and restricted region of gain) at 2p15–16. Selection of 33 BAC clones of 2p15–16 was based on information from National Center of Biotechnology Information (NCBI) (http://www.ncbi.nlm.nih.gov/). Each clone was placed contiguously between BAC clones RP11–518G12 and RP11–511I11 according to the mapping position obtained from the NCBI. These clones were obtained from the BAC/PAC Resource Center at the Children's Hospital Oakland Research Institute. BAC were then isolated from their bacterial cultures with the relevant antibiotics and extracted with a plasmid Mini-Kit (Qiagen, Valencia, CA, USA). The exact location of each clone was determined by means of standard fluorescence in site hybridization (FISH) analysis. Degenerate oligonucleotide-primed polymerase chain reaction (DOP-PCR)[20] was carried out on the DNA of BAC clones, as described elsewhere.[8] DOP-PCR products were dissolved in 30 μL of TE (100 mM Tris-HCl and 1 mM ethylenediaminetetracetic acid, pH 7.5) buffer, and 10 μL of Solution I (Takara Bio, Tokyo, Japan) was added to each of the products, which were then spotted in triplicate onto Hubble-activated slides (Takara Bio) using the Stampman Arrayer (Nippon Laser and Electronics Laboratory, Nagoya, Japan) with a split pin. Slides were fixed in 0.2% sodium dodecylsulfate for 2 min and in 0.3 M NaOH for 5 min, then dehydrated with 100% cold ethanol for 3 min, and finally air-dried. DNA preparation, labeling, array fabrication and hybridization were carried out according to methods described previously.[6,8,21,22] The Agilent Micro Array Scanner (Agilent Technologies, Palo Alto, CA, USA) was used for scanning analysis. The array images thus acquired were further analyzed with Genepix Pro 4.1 (Axon Instruments, Foster City, CA, USA).

Reverse transcription–polymerase chain reaction analysis for screening of candidate genes

The RC-K8 cell line was established from histiocytic lymphoma cells (kindly provided by I. Kubonishi, Kochi, Japan).[23] The L428 cell line was established from Hodgkin's lymphoma (German Collection of Microorganisms and Cell Cultures, Braunschweig, Germany).[24] The Karpas-1106p cell line was established from mediastinal lymphoblastic B-cell lymphoma (kindly provided by A. Karpas, Cambridge, UK).[25] These cell lines and human placenta[26] were subjected to reverse transcription–polymerase chain reaction (RT-PCR) analysis. SuperScript II (Gibco-BRL, Gaithersburg, MD, USA) was used for cDNA. Each 5 μg of total RNA was reverse-transcribed into cDNA in a volume of 40 μL distilled water. RT-PCR was carried out for nine genes by using the specific corresponding primers. The names and accession numbers of the genes were: *LOC442017* (XM_497839), *LOC130865* (XM_497840), *ATP1B3P1* (NG_000849), *PAPOLG* (NM_022894), *LOC400957* (XM_379097), *REL* (NM_002908), *LOC344423* (AK124741), *FLJ32312* (NM_144709) and *PEX13* (NM_002618). The primers used for RT-PCR are shown in Table 1. Each primer was designed so that the melting temperature (Tm) value would be between 58°C and 63°C. Amplifications were carried out using a Thermal Cycler (Perkin-Elmer, Norwalk, CT, USA), and RT-PCR was carried out using the touchdown PCR method. The reactions comprised 10 cycles of denaturation (94°C, 0.5 min), annealing (65°C, 0.5 min, 1°C decrease per 2 cycles) and extension (72°C, 2.5 min), followed by 35 cycles of denaturation (94°C, 0.5 min), annealing (60°C, 0.5 min) and extension (72°C, 2.5 min), and a final extension of 5 min at 72°C. In the cases of *LOC130865* and *LOC442017*, annealing temperature of the reaction ranged from 63 to 58°C.

Real-time quantitative–polymerase chain reaction

Expression levels of *REL*, *BCL11A*, *LOC344423* and *PEX13* mRNA were measured by means of real-time fluorescence detection using a previously described method.[22,27] Briefly, the primers of *REL* were sense: 5′-cccacgctcaggcaataca-3′ and antisense: 5′-tggtgggataccttgcgaat-3′, those of *BCL11A* were sense: 5′-aaaaagagagaaacaaaaaagtgtgaca-3′ and antisense: 5′-catccatgtgacattctagcagg-3′, those of *LOC344423* were sense: 5′- gccatgcactagagggtactca-3′ and antisense: 5′-gctcttcttgacacctcatcaa-3′, and those of *PEX13* were sense: 5′-aggaccgagcagctacctca-3′ and antisense: 5′-tggcaa-ctacatggtcatcctc-3′. Real-time PCR using SYBR® Green1 and primers was carried out with a Smart Cycler System (Takara Bio) according to the manufacturer's protocol. *G6PDH* served as an endogenous control, whereas the expression

Table 1. Reverse transcription–polymerase chain reaction analysis of genes within the 2p15–16 amplification region of RC-K8, L428 and Karpas-1106p

Gene	Forward primer	Reverse primer	Human placenta	RC-K8	L428	Karpas 1106p
LOC442017	5′-ctgtccaaaccgtcttcactc	5′-acttggcagtggaggcgtag	+/–	–	–	+/–
LOC130865	5′-cccacactcgcagaaagatt	5′-acagggacagctatgctgttag	+/–	+/–	+/–	+
ATP1B3P1	5′-gcacacgatgaagaaggagtc	5′-gcttgaagtaacgaaatgggagat	+/–	+/–	+/–	–
PAPOLG	5′-attgacgccatgaaaccatt	5′-gcttctcaggcgagagtcgt	+	+	+	–
LOC400957	5′-actatagccggatacagggaga	5′-cgtagcacccgttacacaga	+/–	+	+/–	–
REL	5′-gaaactgtgccaggatcacg	5′-ccaacaggtattctcaggaatgg	+	++	++	++
LOC344423	5′-catgatggcctagcatatgaa	5′-gctcttcttgacacctcatcaa	+	++	++	++
FLJ32312	5′-tctgttagtcatgttggaagcact	5′-ggctttcataactgccattcta	+/–	–	+	+
PEX13	5′-acaaccgcctccgtgtaga	5′-ctctggcaactacatggtcatc	+	++	++	++

Detected by electrohphoresis: ++, positive thick band; +, positive thin band; +/–, very weakly positive band; –, no band.

doi: 10.1111/j.1349-7006.2006.00209.x
© 2006 Japanese Cancer Association

levels of *REL*, *BCL11A*, *LOC344423* and *PEX13* mRNA in each sample were normalized on the basis of the corresponding *G6PDH* content and recorded as relative expression levels. Overexpression was defined as the mean of the relative expression plus two or more standard deviation units.

Results

Recurrent amplification detected by genome-wide array-CGH at 2p15–16 in DLBCL

Genome-wide array-CGH analysis at a resolution of 1.3 Mb showed that 25 of the 99 DLBCL cases (25%) had copy number gains on chromosome 2p. All cases included recurrent copy number gain at 2p15–16, with three of the 25 cases showing genomic amplification ($\log_2$ ratio ≥ 1). Individual genomic profiles of these three tumors (D768, D778 and D792) showed that every amplification was located at 2p15–16 (Fig. 1). The common recurrent region of the 25 cases was confined to the 4.5-Mb region at 2p15–16 (Fig. 2).

Determination of minimal common region by contig array-CGH

We speculated that the target genes of 2p15–16 amplification were located within the common recurrent region between BAC clones RP11–518G12 and RP11–511I11. To specify the alterations of 2p15–16 in more detail, we prepared high-resolution contig array glass slides containing 33 BAC clones, which were placed contiguously throughout the 4.5-Mb region. Contig array-CGH was conducted for seven cases, for which the genome-wide array-CGH showed gain or amplification at 2p15–16 (Fig. 3). The profiles showed that the common region for three cases with amplification ($\log_2$ ratio ≥ 1.0) was 1.6 Mb located between BAC clones RP11–440P5 and RP11–813L21. Further analysis for four cases with genomic gain confined the minimal common region to 500 kb between BAC clones RP11–416L21 and RP11–373L24. The region contained only *REL*, not *BCL11A*, as the candidate oncogene.

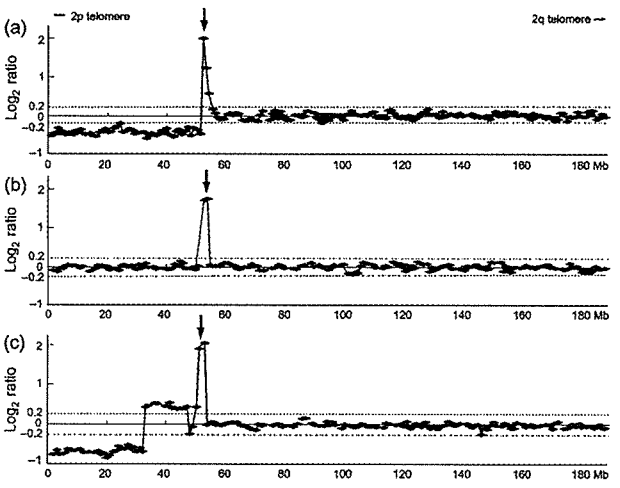

Fig. 1. Representative individual genomic profiles of chromosome 2 in diffuse large B-cell lymphoma. Genome-wide array-based comparative genomic hybridization profiles of three cases with 2p amplification: (a) D768, (b) D778 and (c) D792. Dots represent the $\log_2$ ratio of bacterial artificial chromosome/P-1-derived artificial chromosome clones, which are shown in order from the p telomere to the q telomere. The vertical arrow above each profile indicates the region of amplification. The threshold for gain and loss was defined as the $\log_2$ ratio of +0.2 and −0.2, respectively.

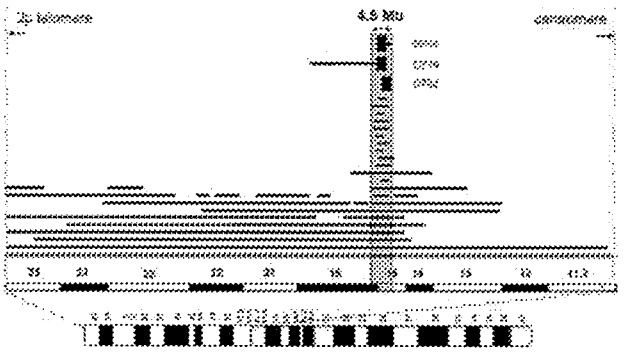

Fig. 2. Illustration of genomic amplification at chromosome 2p. Summary of genome-wide array-based comparative genomic hybridization profiles at 2p. Copy number gains were detected in 25 of 99 diffuse large B-cell lymphoma cases. Thin lines: low copy number gain ($+0.2 \leq \log_2$ ratio $< +1.0$); thick lines: high copy number gain (amplification, $\log_2$ ratio $\geq +1.0$). Genomic amplifications were observed at 2p15–16 in three cases (D768, D778 and D792). The gray area represents the most common recurrent region in the 25 cases, which is 4.5 Mb in length.

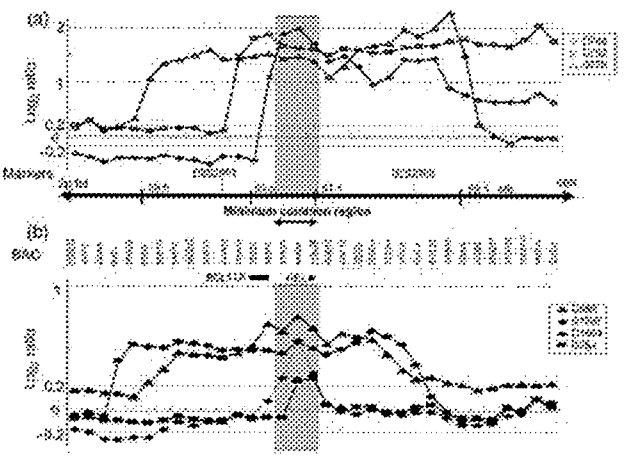

Fig. 3. Contig array-based comparative genomic hybridization (array-CGH) profiles at 2p15–16 in diffuse large B-cell lymphoma. Contig array-CGH containing 33 bacterial artificial chromosome (BAC) clones were constructed and placed contiguously at the most common recurrent region (4.5 Mb) identified with genome-wide array-CGH. (a) Genomic profiles of three cases with high copy number gain ($\log_2$ ratio $\geq +1.0$) at 2p15–16. (b) Genomic profiles for four cases with low copy number gain ($+0.2 \leq \log_2$ ratio $< +1.0$) at 2p15–16. Dots represent the $\log_2$ ratio of BAC clones, which are shown in order from the p telomere to the centromere. Vertical lines: $\log_2$ ratio. The thresholds for gain and loss were defined as the $\log_2$ ratio of +0.2 and −0.2, respectively. The BAC clones are all shown contiguously. The underlined BAC clones were used for genome-wide array-CGH. The gray area represents the minimum common region in the 25 cases, which is 500-kb in length between BAC clones RP11–416L21 and RP11–373L24.

© 2006 Japanese Cancer Association

Relationship between genomic alteration and expression of *REL* and *BCL11A*

Four of the seven cases analyzed by contig array-CGH showed gain or amplification for both *REL* and *BCL11A* genes, whereas the remaining three demonstrated gain or amplification of *REL* alone (Fig. 4a). To investigate the relationship between genomic amplification and gene expression, we conducted RQ-PCR analysis for both candidate genes in six of the seven cases with 2p15–16 gain whose RNA was available, and in seven cases without any change at 2p15–16 (Fig. 4b). Three cases with copy number gains for both genes (D778, D856 and D1767) demonstrated overexpression for both, and two cases with a copy number gain of *REL* alone (D768 and D1664) showed significant overexpression of *REL*, but the remaining case (D754) showed an expression level beyond the average for normal controls, although the difference was not significant. These three cases showed neither genomic gain nor overexpression of *BCL11A* (D768, D1664 and D754). Correlation coefficients for the $\log_2$ ratio of DNA and the relative amount of mRNA were 0.76 for *REL* and 0.89 for *BCL11A*. These data indicate that overexpression of *REL* and *BCL11A* correlates well with the level of genomic amplification of both genes. Thus, both of these two genes are targets at the 2p15–16 region, whose expression is altered by genomic amplification in DLBCL. Furthermore, we also conducted RQ-PCR in an additional six DLBCL cases with 2p gain, for which contig array-CGH could not be carried out. All of the additional cases except one showed *REL* overexpression in accordance with genomic gain, whereas only four cases showed *BCL11A* overexpression (data not shown).

RT-PCR analysis of the genes within the 2p15–16 amplicon, and RQ-PCR for *LOC344423* and *PEX13*

The contig array-CGH showed that nine genes were located within the 2p15–16 minimum common region (500 kb in length). RT-PCR analysis was used to evaluate expression of these nine genes (Table 1). The cell lines used for screening were B-cell lymphoma cell lines with 2p amplification (RC-K8, L428[28] and Karpas-1106p[29]) and human placenta. The sizes of all products obtained by RT-PCR were confirmed by electrophoresis and were as expected (data not shown). Expression of three genes (*REL*, *LOC344423* and *PEX13*) could be detected in all B-cell lymphoma cell lines with 2p amplification. We conducted RQ-PCR analysis for *LOC344423* and *PEX13* in the same six cases with 2p15–16 gain to investigate the relationship between genomic amplification and gene expression (Fig. 4c,d). All cases but one showed overexpression of *LOC344423* and *PEX13* in a similar fashion to that of *REL*. Correlation coefficients for the $\log_2$ ratio of DNA and the relative amount of mRNA were 0.73 for *LOC344423* and 0.97 for *PEX13*. Thus, both of these genes are also possible targets in the 2p15–16 region in DLBCL, although functional study is needed.

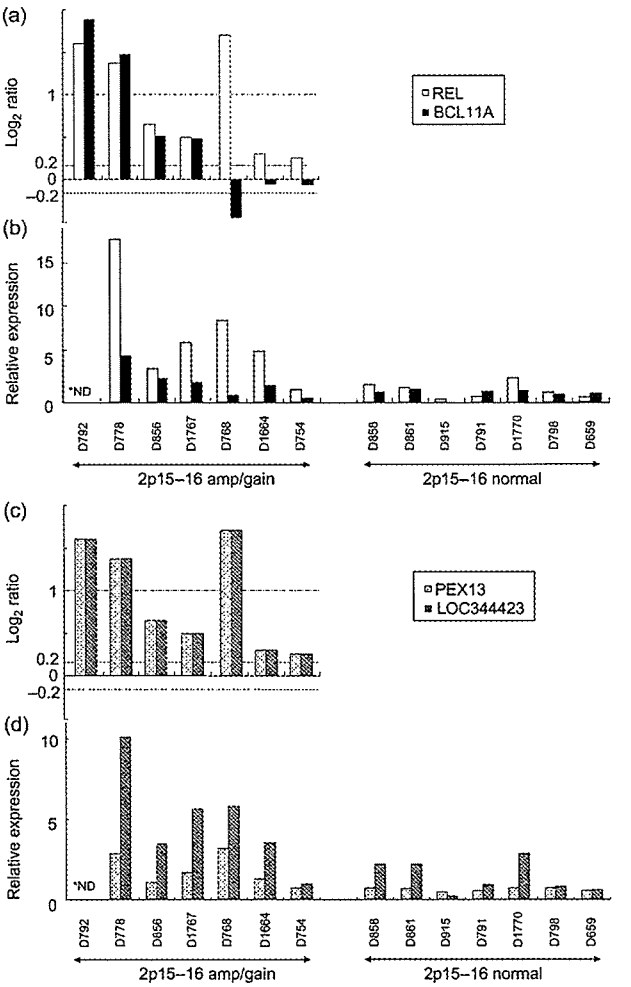

Fig. 4. Relationship between genomic amplification and expression of *REL*, *BCL11A*, *PEX13* and *LOC344423*. (a) Mean $\log_2$ ratio of all bacterial artificial chromosome (BAC) clones containing the *REL* locus and the *BCL11A* locus obtained from contig array-based comparative genomic hybridization (array-CGH). The thresholds for gain and loss were defined as the $\log_2$ ratio of +0.2 and –0.2, respectively. White bars: *REL* locus. Black bars: *BCL11A* locus. (b) Relative expression levels of *REL* and *BCL11A* determined by real-time quantitative-polymerase chain reaction (RQ-PCR) in cases with 2p15–16 gain and those without any change at 2p15–16 (normal). For relative expression levels, each expression was normalized on the basis of the corresponding *G6PDH* content. White bars: *REL*. Black bars: *BCL11A*. *ND: RQ-PCR not done for D792 because RNA was not available. (c) Mean $\log_2$ ratio of all BAC clones containing the *PEX13* locus and the *LOC344423* locus obtained from contig array CGH. The thresholds for gain and loss were defined as the $\log_2$ ratio of +0.2 and –0.2, respectively. Dotted bars: *PEX13* locus. Striped bars: *LOC344423* locus. (d) Relative expression levels of *PEX13* and *LOC344423* detected by RQ-PCR in cases with 2p15–16 gain and of cases without any change at 2p15–16 (normal). For relative expression levels, each expression was normalized on the basis of the corresponding *G6PDH* content. Dotted bars: *PEX13*. Striped bars: *LOC344423*. *ND: RQ-PCR not done for D792 because RNA was not available.

Discussion

Gain of chromosome 2p has been identified as a recurrent alteration in 20% of DLBCL,[9–15] 50% of cHL,[16,17] and 3–47% of PMBCL cases.[11,14,15] In previous studies, CGH and FISH analyses were used as tools to investigate genomic alterations. Array-CGH is superior to these two methods in terms of higher resolution and the ability to directly map the copy number changes to the genome sequence. The genome-wide

doi: 10.1111/j.1349-7006.2006.00209.x
© 2006 Japanese Cancer Association

array-CGH with a resolution of 1.3 Mb used for the 99 DLBCL cases enrolled in our study identified a common recurrent 4.5-Mb region at 2p15–16. By carrying out high-resolution contig array-CGH in the recurrent region, we were able to restrict the minimal common region to 500 kb in length.

The *REL* proto-oncogene, which is located in the 2p15–16 region, has been investigated as a target of the region in many reported studies. As *BCL11A* was identified as another oncogene in this region,[30] the two oncogenes have been examined together. In most cHL cases, coamplification of both gene loci was shown by fluorescence immunophenotyping and interphase cytogenetics (FICTION). Bea *et al.* detected simultaneous overexpression of both genes in all DLBCL cases with 2p amplification by means of RQ-PCR.[12]

In the present study, we were able to identify the minimally targeted genomic regions of 2p15–16 amplification where *REL*, not *BCL11A*, is located as the only candidate oncogene. Martin-Subero *et al.* investigated amplification of both gene loci, *REL* and *BCL11A*, in cHL tumors by means of FICTION and reported that one case displayed selective amplification of the *REL* locus and two cases showed signal patterns suggesting breakpoints within the *REL* locus.[16] They concluded that the target of 2p alterations might be closely associated with the *REL* locus, consistent with the region we identified as a minimum common region, although they did not investigate gene expression.

It has been reported that a high copy number of *REL* correlates with extranodal disease in DLBCL.[9] A recent multicenter cooperative study demonstrated that expression of *REL* and *BCL11A* was frequently recognized in the germinal center like B cell (GCB)-DLBCL subgroup that is known to have favorable prognosis. However, the number of cases with 2p gain or amplification in our cohort was too small to draw any definitive conclusions in this respect, but it has been reported that the correlation of 2p gain and favorable outcome could not be demonstrated.[15]

To investigate the correlation between genomic amplification and expression, we carried out RQ-PCR analysis of the candidate genes *REL* and *BCL11A* and found a significant correlation between genomic alteration and expression in both genes. This indicates that both genes are common targets for genomic amplification in this region. However, given the fact that *REL* is more frequently amplified than *BCL11A*, it is speculated that *REL* may play a more important role than *BCL11A* in the development of lymphoma.

Our results identified two additional candidate genes as targets of the 2p15–16 amplicon and demonstrated for the first time the overexpression of *LOC344423 and PEX13* in primary tumors. Because these two genes and *REL* are located within the same BAC (RP11–373L24), it is speculated that the *LOC344423* and *PEX13* loci are also amplified in cases with *REL* locus amplification. However, the coding frame of *LOC344423* is missing nor regulatory RNA, such as micro RNA, is found, and *PEX13* is a structural gene of the peroxisome. This suggests that neither *LOC344423* nor *PEX13* are likely candidate genes for oncogenesis.

Acknowledgments

We are grateful to Dr Yoshitaka Hosokawa, Dr Shinobu Tsuzuki and Dr Ritsuro Suzuki for their discussions and encouragement throughout this study. The outstanding technical assistance of Ms Hiroko Suzuki is very much appreciated. This work was supported in part by Grants-in-Aid from the Ministry of Health, Labor and Welfare, from the Ministry of Education, Culture, Sports Science and Technology, from the Japan Society for the Promotion of Science, and from the Foundation of Promotion of Cancer Research, as well as by a Grant-in-Aid for cancer research from the Princess Takamatsu Cancer Research Fund (03-23503) and the Wella Award from the Japan Leukemia Research Fund awarded to MS.

References

1 The Non-Hodgkin's Lymphoma Classification Project. A clinical evaluation of the International Lymphoma Study Group Classification of non-hodgkin's lymphoma. *Blood* 1997; **89**: 3909–18.
2 Harris NL, Jaffe ES, Stein H *et al.* A revised European–American classification of lymphoid neoplasms: a proposal from the International Lymphoma Study Group. *Blood* 1994; **84**: 1361–92.
3 Offit K, Le Coco F, Louie DC *et al.* Rearrangement of *BCL6* gene as a prognostic marker in diffuse large cell lymphoma. *N Engl J Med* 1994; **331**: 74–80.
4 Kramer MHH, Hermans J, Wijburg E *et al.* Clinical relevance of BCL2, BCL6, and MYC rearrangements in diffuse large B-cell lymphoma. *Blood* 1998; **92**: 3152–62.
5 Gatter KC, Warnke RA. Diffuse large B-cell lymphoma. In Jaffe ES, Harris NL, Stein H, Vardiman JW, eds. *World Health Classification of Tumors. Pathology and Genetics of Tumors of Haematopoietic and Lymphoid Tissues*. Washington: IARC Press, Lyon, 2001; 171–4.
6 Tagawa H, Tsuzuki S, Suzuki R *et al.* Genome-wide array-based comparative genomic hybridization of diffuse large B-cell lymphoma: comparison between CD5-positive and CD5-negative cases. *Cancer Res* 2004; **64**: 5948–55.
7 Tagawa H, Suguro M, Tsuzuki S *et al.* Comparison of genome profiles for identification of distinct subgroups of diffuse large B-cell lymphoma. *Blood* 2005; **106**: 1770–7.
8 Ota A, Tagawa H, Karnan S *et al.* Identification and characterization of a novel gene, *C13orf25*, as a target for 13q31-q32 amplification in malignant lymphoma. *Cancer Res* 2004; **64**: 3087–95.
9 Houldsworth J, Mathew S, Rao PH *et al.* *REL* proto-oncogene is frequently amplified in extranodal diffuse large cell lymphoma. *Blood* 1996; **87**: 25–9.
10 Rao PH, Houldsworth J, Dyomina K *et al.* Chromosomal and gene amplification in diffuse large B-cell lymphoma. *Blood* 1998; **92**: 234–40.
11 Palanisamy N, Abou-Elella AA, Chaganti SR *et al.* Similar patterns of genomic alterations characterize primary mediastinal large B-cell lymphoma and diffuse large B-cell lymphoma. *Genes Chromosomes Cancer* 2002; **33**: 114–22.
12 Bea S, Colomo L, Lopez-Guillermo A *et al.* Clinicopathologic significance and prognostic value of chromosomal imbalances in diffuse large B-cell lymphomas. *J Clin Oncol* 2004; **22**: 3498–506.
13 Houldsworth J, Olshen AB, Cattoretti G *et al.* Relationship between *REL* amplification, REL function, and clinical and biologic features in diffuse large B-cell lymphomas. *Blood* 2004; **103**: 1862–8.
14 Feuerhake F, Kutok JL, Monti S *et al.* NFκB activity, function, and target-gene signatures in primary mediastinal large B-cell lymphoma and diffuse large B-cell lymphoma subtypes. *Blood* 2005; **106**: 1392–9.
15 Bea S, Zettl A, Wright G *et al.* Diffuse large B-cell lymphoma subgroups have distinct genetic profiles that influence tumor biology and improve gene expression-based survival prediction. *Blood* 2005; **106**: 3183–90.
16 Martin-Subero JI, Gesk S, Harder L *et al.* Recurrent involvement of the *REL* and *BCL11A* loci in classical Hodgkin lymphoma. *Blood* 2002; **99**: 1474–7.
17 Joos S, Menz CK, Wrobel G *et al.* Classical Hodgkin lymphoma is characterized by recurrent copy number gains of the short arm of chromosome 2. *Blood* 2002; **99**: 1381–7.

© 2006 Japanese Cancer Association

18 Goff LK, Neal MJ, Crawley CR *et al.* The use of real-time quantitative polymerase chain reaction and comparative genomic hybridization to identify amplification of the *REL* gene in follicular lymphoma. *Br J Haematol* 2000; **111**: 618–25.
19 Pinkel D, Segraves R, Sudar D *et al.* High resolution analysis of DNA copy number variation using comparative genomic hybridization to microarrays. *Nat Genet* 1998; **20**: 207–11.
20 Telenius H, Carter NP, Bebb CE *et al.* Degenerate oligonucleotide-primed PCR: general amplification of target DNA by a single degenerate primer. *Genomics* 1992; **13**: 718–25.
21 Kameoka Y, Tagawa H, Tsuzuki S *et al.* Contig array CGH at 3p14.2 points to the *FRA3B/FHIT* common fragile region as the target gene in diffuse large B cell lymphoma. *Oncogene* 2004; **23**: 9148–54.
22 Kasugai Y, Tagawa H, Kameoka Y, Morishima Y, Nakamura S, Seto M. Identification of *CCND3* and *BYSL* as candidate targets for 6p21 amplification in diffuse large B-cell lymphoma. *Clin Cancer Res* 2005; **11**: 8265–72.
23 Kubonishi I, Niiya K, Miyoshi I. Establishment of a new human lymphoma line that secretes plasminogen activator. *Jpn J Cancer Res* 1985; **76**: 12–15.
24 Schaadt M, Fonatsch C, Kirchner H, Diehl V. Establishment of a malignant, Epstein–Barr virus (EBV)-negative cell-line from the pleura effusion of a patient with Hodgkin's disease. *Blut* 1979; **38**: 185–90.
25 Nacheva E, Dyer MJ, Metivier C *et al.* B-cell non-Hodgkin's lymphoma cell line (Karpas 1106) with complex translocation involving 18q21.3 but lacking *BCL2* rearrangement and expression. *Blood* 1994; **84**: 3422–8.
26 Takizawa J, Suzuki R, Kuroda H *et al.* Expression of the *TCL1* gene at 14q32 in B-cell malignancies but not in adult T-cell leukemia. *Jpn J Cancer Res* 1998; **89**: 712–18.
27 Suguro-Katayama M, Suzuki R, Kasugai Y *et al.* Heterogeneous copy numbers of API2-MALT1 chimeric transcripts in mucosa-associated lymphoid tissue lymphoma. *Leukemia* 2003; **17**: 2508–12.
28 Joos S, Granzow M, Holtgreve-Grez H *et al.* Hodgkin's lymphoma cell lines are characterized by frequent aberrations on chromosomes 2p and 9p including *REL* and *JAK2*. *Int J Cancer* 2003; **103**: 489–95.
29 Joos S, Otano-Joos MI, Ziegler S *et al.* Primary mediastinal (thymic) B-cell lymphoma is characterized by gains of chromosomal material including 9p and amplification of the *REL* gene. *Blood* 1996; **87**: 1571–8.
30 Satterwhite E, Sonoki T, Willis TG *et al.* The *BCL11* gene family: involvement of *BCL11A* in lymphoid malignancies. *Blood* 2001; **98**: 3413–20.

doi: 10.1111/j.1349-7006.2006.00209.x
© 2006 Japanese Cancer Association

Randomized phase II study of concurrent and sequential rituximab and CHOP chemotherapy in untreated indolent B-cell lymphoma

Michinori Ogura,[1,9] Yasuo Morishima,[1] Yoshitoyo Kagami,[1] Takashi Watanabe,[2] Kuniaki Itoh,[3] Tadahiko Igarashi,[3] Tomomitsu Hotta,[4] Tomohiro Kinoshita,[5] Yasuo Ohashi,[6] Shigeo Mori,[7] Takashi Terauchi[8] and Kensei Tobinai[2]

[1]Department of Hematology and Cell Therapy, Aichi Cancer Center, 1-1 Kanokoden, Chikusa-ku, Nagoya 464-8681; [2]Hematology and Stem Cell Transplantation Division, National Cancer Center Hospital, 5-1-1 Tsukiji, Chuo-ku, Tokyo 104-0045; [3]Hematology and Oncology Division, National Cancer Center Hospital East, 6-5-1 Kashiwanoha, Kashiwa, Chiba 277-8577; [4]Department of Hematology and Oncology, Tokai University School of Medicine, Bohseidai, Isehara, Kanagawa 259-1193; [5]First Department of Internal Medicine, Nagoya University School of Medicine, Nagoya 466-8560; [6]Biostatistics Sciences, School of Health Science and Nursing Biostatistics, University of Tokyo, 7-3-1 Hongo, Bunkyo-ku, Tokyo 113-8655; [7]Department of Pathology, Institute of Medical Science, University of Tokyo, Shirokanedai, Minato-ku, Tokyo 108-8639; and [8]Research Center for Cancer Prevention and Screening, National Cancer Center, 5-1-1 Tsukiji, Chuo-ku, Tokyo 104-0045, Japan

(Received October 16, 2005/Revised December 26, 2005/Accepted December 26, 2005/Online publication March 30, 2006)

CHOP combined with rituximab (R-CHOP) is regarded as one of the most effective treatments for indolent B-cell non-Hodgkin lymphoma (B-NHL), however, its optimal combination schedule remains unknown. We performed a randomized phase II study to explore a more promising schedule in untreated, advanced indolent B-NHL. Patients were randomized to receive either six courses of CHOP concurrently with rituximab (Arm C), or six courses of CHOP followed by six courses of weekly rituximab (Arm S). A total of 69 patients received the concurrent (n = 34) or sequential (n = 35) regimen. Overall response rate (ORR) in Arm C was 94% (95% confidence interval [CI], 79 to 99), including a 66% complete response (CR) compared with 97% (95% CI, 85–100), including a 68% CR in Arm S. Patients in Arm C experienced more grade 4 neutropenia (85% *versus* 70%) and experienced more grade 3 or greater non-hematological toxicities (21% *versus* 12%). Both arms were tolerated well. With a median follow-up of 28.2 months, the median progression-free survival (PFS) time was 34.2 months in Arm C, and was not reached in Arm S. R-CHOP is highly effective in untreated indolent B-NHL, either concurrent or in a sequential combination. Both combination schedules deserve further investigation. (*Cancer Sci* 2006; 97: 305–312)

Indolent non-Hodgkin lymphomas (NHLs), in which the representative type of lymphoma is follicular lymphoma (FL), are characterized by an advanced stage at presentation, lack of symptoms associated with the disease, and indolent behavior in terms of the time to symptomatic disease progression.[1,2] Although many chemotherapeutic agents and combination therapies are used in the treatment of patients with FL, a large majority of these patients remain incurable.[3–5] Thus, more effective strategies are needed to overcome the current therapeutic limitations. Rituximab is a chimeric monoclonal anti-CD20 antibody that can deplete malignant B cells through complement-dependent cytotoxicity, antibody-dependent cell-mediated cytotoxicity (ADCC),[6] and apoptotic mechanisms.[7] It has also been shown to sensitize lymphoma cell lines resistant to cytotoxic drugs.[8] In recent years, it was demonstrated that rituximab is an active agent against indolent B-NHL and has become a standard component of first-line therapy, either as a single agent or in combination with chemotherapy.[9–18] Recently, the addition of rituximab to the cyclophosphamide, doxorubicin, vincristine and prednisolone (CHOP) regimen or cyclophosphamide, vincristine and prednisolone (CVP) regimen was demonstrated to improve the clinical outcome in patients with previously untreated advanced FL, without increased toxicity. Czuczman *et al.* conducted the first phase II study on the combination of rituximab with CHOP in mostly untreated patients with low-grade B-NHL or FL.[14] They treated the patients with six cycles of standard CHOP given at 3-week intervals along with rituximab administered twice before, during and after the six cycles of CHOP therapy. All treated patients (n = 38) responded with a complete response (CR) rate of 87%, and the median time to progression (TTP) was 82.3 months.[15] Marcus *et al.* reported significant superiority of CVP plus rituximab (R-CVP) over CVP for previously untreated patients with advanced FL in a randomized phase III study.[18] From the viewpoint of the possible synergistic effect between rituximab and chemotherapeutic drugs, it seems to be reasonable that rituximab be delivered in combination with chemotherapeutic drugs concurrently. Whereas, from the viewpoint of enhancing the ADCC effect, which is one of the putative antitumor mechanisms of rituximab, it seems reasonable that rituximab be administered in situations in which effector cells such as macrophages, natural killer cells and neutrophils are intact, in other words, there are no cytotoxic or immunosuppressive effects of chemotherapeutic drugs. Thus, to maximize the

[9]To whom correspondence should be addressed. E-mail: mi-ogura@naa.att.ne.jp
Present address: The Department of Hematology, Nagoya Daini Red Cross Hospital, 2-9, Myokencho, Showaku, Nagoya 466-8650, Japan.
Portions of this study were presented at the Annual Meeting of the American Society of Clinical Oncology, New Orleans, 2004.

doi: 10.1111/j.1349-7006.2006.00173.x
© 2006 Japanese Cancer Association

possible ADCC effect, it might be preferable that rituximab be delivered to patients after recovery from the toxic or immunosuppressive effect of chemotherapy. However, the optimal schedule for the combined use of rituximab and chemotherapy remains unclear. To explore a more promising regimen of rituximab combined with CHOP therapy for the treatment of indolent B-cell NHL, we conducted a randomized phase II trial.

Materials and Methods

Patients

Between July 1999 and July 2000, 69 patients with newly diagnosed indolent B-cell NHLs were enrolled. Eligibility criteria included: aged between 20 and 70 years; a histopathological diagnosis of indolent B-NHL according to the Revised European-American Lymphoma (REAL) classification[19] (including small lymphocytic lymphoma, lymphoplasmacytic lymphoma, FL or marginal zone B-cell lymphoma); no previous treatment; stages III or IV disease according to the Ann Arbor staging system;[20] CD20 positive lymphomas confirmed by immunohistochemistry or flow cytometry; an Eastern Cooperative Oncology Group (ECOG)[21] performance status (PS) of 0, 1 or 2; negative for the hepatitis B virus surface antigen, hepatitis C virus antibody or human immunodeficiency virus antibody; having no other malignancies and normal renal, pulmonary and hepatic function. Approval was obtained from the local institutional review boards of all participating institutions. Informed consent was obtained from all patients before enrollment in accordance with the Declaration of Helsinki.

Study design

This randomized phase II study was designed as a two arm parallel phase II study. The expected overall response rate (ORR) (P1) for either arm was set at 95% based on the phase II study by Czuczman *et al.* where CHOP was combined with rituximab,[14] while the threshold response rate (P0) was set at 75%, based on previous reports on CVP or COP, CHOP or CHOP-like studies.[22] The number of patients required for this study was 27 per arm, calculated in accordance with Fleming's two-stage testing procedure,[23] at $\alpha = 0.05$ (two-side) and $1-\beta = 0.8$. Assuming that up to 20% of patients might be ineligible due to inaccurate histopathological diagnosis at participating institutions, we planned to enroll at least 34 patients per arm. From the viewpoint of selection design by Simon *et al.*,[24] the selection of one arm showing a 15% higher percentage CR at 90% probability would be possible with this number of patients, if the percentage CR of both arms would achieve at least 65%.

Treatment schedule

Patients fulfilling the inclusion criteria were randomly assigned to either the concurrent arm (Arm C) or sequential arm (Arm S) at the independent randomization center, thereby minimizing the bias between the arms regarding PS, clinical stage and institution. All patients were treated with six courses of standard CHOP chemotherapy (cyclophosphamide 750 mg/m^2, i.v., day 1; doxorubicin 50 mg/m^2 i.v., day 1; vincristine 1.4 mg/m^2 [capped at 2 mg] i.v., day 1; and prednisolone 100 mg, p.o., days 1–5) every 3 weeks. In addition, patients allocated to Arm C received rituximab (375 mg/m^2 i.v.) 2 days prior to each CHOP cycle, whereas patients allocated to Arm S received rituximab (375 mg/m^2, weekly six times, i.v.) 4 weeks after completion of the sixth cycle of CHOP. Rituximab was given intravenously based on the preceding phase I study in Japan.[25]

Patient evaluation, end-points and response criteria

Patients were observed until the progression of lymphomas or death. Tumor restaging was performed at approximately 3-monthly intervals for the first 12 months and every 4 to 6 months thereafter.

The primary end-point of this study was an ORR in all eligible patients, that is, the percentage of patients achieving a CR, CRu, or partial response (PR), evaluated according to the International Workshop Response Criteria for NHL.[26] CR required the disappearance of all detectable clinical and radiographic evidence of disease, disappearance of disease-related symptoms, and normalization of biochemical abnormalities. Adenopathy on computed tomography (CT) scans must have regressed to normal size (1.5 cm or less in the greatest transverse diameter). CRu was defined as complete disappearance of all detectable clinical and radiographic abnormalities of the disease, with the exception of the presence of a residual adenopathy larger than 1.5 cm, as long as the sum of products of the greatest diameters (SPDs) of the adenopathy had decreased by more than 75%. Residual bone marrow abnormalities, that included increased number or size of lymphoid aggregates without definite cytological evidence of persistent lymphoma, could also be present in patients in the CRu response category. PR was defined as a greater than 50% decrease in the SPDs of the largest dominant nodes or nodal masses. Stable disease patients were defined as having any response that was less than a PR or an increase in the SPDs by less than 25%, with no new lesions appearing. Progressive disease was defined by an increase of more than 25% in the size of the SPDs of the measured lesions, or the appearance of new lesions. All cases were centrally reviewed radiographically using CT films.

Secondary end-points were percentage CR, including percentage CRu and a progression-free survival (PFS) for all eligible patients, as an interval from the day of enrollment to the first day when tumor progression or death due to any cause was observed. The response to the combined regimen and PFS period for each patient was evaluated until at least 2 and a half years after the completion of treatment.

Adverse events (AEs) were graded according to the toxicity criteria of the Japan Clinical Oncology Group,[27] an expanded version of the Common Toxicity Criteria of the National Cancer Institute (version 1.0).

Human antichimeric antibody assay and pharmacokinetics of rituximab

Serum human antichimeric antibody (HACA) levels were monitored at 8 and 10 months after treatment initiation using an enzyme-linked immunosorbent assay (ELISA), as described previously.[28]

Serum rituximab levels were monitored using ELISA for patients who signed another informed consent form to participate in this pharmacokinetic (PK) study. The PK parameters were calculated using WinNonlin PK software (WinNonlin

doi: 10.1111/j.1349-7006.2006.00173.x
© 2006 Japanese Cancer Association

Standard Japanese Edition, version 1.1; Scientific Consulting, Apex, NC, USA).

Statistical methods

The ORR, percentage CR, and their 95% confidence intervals (CIs) were calculated with per protocol sets (PPS) of data for all eligible patients and full analysis sets (FAS) of data for all enrolled patients under the F-distribution. The median PFS time, time to CR (TTCR) and time to response (TTR), and their 95% CIs were estimated for all eligible and evaluative patients using the method of Kaplan and Meier, and were compared using the log–rank test. In addition, pretreatment factors affecting the ORR and PFS were analyzed for all eligible and evaluative patients by univariate and multivariate analyses using Fisher's exact test, Wilcoxon's rank sum test, the log–rank test, the logistic regression model or Cox's proportional hazard regression model.

All statistical analyses were performed using SAS software (version 6.12; SAS Institute, Cary, NC, USA). Data used for theses analyses were finally confirmed on March 31, 2004.

Results

Patient characteristics

A total of 69 patients were enrolled from 21 institutions (see Appendix I); 34 patients were allocated to Arm C and 35 patients to Arm S. Patient characteristics at study entry are summarized in Table 1. The median age was 52 years (range, 26–69 years). The major characteristics of the two arms were very similar in both the enrolled and eligible patients. Retrospectively, we analyzed the Follicular Lymphoma International Prognostic Index (FLIPI) in all patients.[29] FLIPI was equally distributed between the two arms. Twenty-eight patients (82%) in Arm C and 30 patients (86%) in Arm S were judged

Table 1. Patient characteristics

Factor	Enrolled (n = 69)			Eligible (n = 66)		
	Arm C	Arm S	Total	Arm C	Arm S	Total
Sex						
Female	18	18	36	17	18	35
Male	16	17	33	15	16	31
Age (years)						
Median	53	50	52	54.5	49.5	52.5
Range	36–65	26–69	26–69	36–65	26–69	26–69
Performance status (ECOG)						
0	29	30	59	28	29	57
1	5	5	10	4	5	9
Histopathology (REAL)†						
Follicular, grade 1	12	11	23	11	11	22
Follicular, grade 2	21	19	40	20	19	39
Follicular, grade 3	0	2	2	0	2	2
Marginal zone B-cell	1	0	1	1	0	1
Low grade B-NHL, NOS‡	0	2	2	0	2	2
No specimen submitted§	0	1	1	0	0	0
Clinical stage (Ann Arbor)						
III	14	15	29	13	14	27
IV	20	20	40	19	20	39
B-symptoms						
Absent	30	33	63	29	32	61
Present	4	2	6	3	2	5
LDH						
Normal	32	31	63	31	30	61
Elevated	2	4	6	1	4	5
No. of extranodal sites						
0–1	25	26	51	24	25	49
≤2	9	9	18	8	9	17
International Prognostic Index						
Low	21	21	42	21	20	41
Low-intermediate	12	12	24	10	12	22
High-intermediate	1	1	2	1	1	2
High	0	1	1	0	1	1
Follicular Lymphoma International Prognostic Index						
Low	16	15	31	16	15	31
Intermediate	12	15	27	10	14	25
High	6	5	11	5	5	10

†According to the diagnosis by the central pathology review. ‡Low-grade B-cell non-Hodgkin lymphoma (NHL) not otherwise specified. §Specimen was not submitted to the central pathology review. LDH, lactic dehydrogenase.

© 2006 Japanese Cancer Association

Table 2. Response to therapy

Arm		n	No. of patients achieving response						Response rate (95% CI)	
			CR	CRu	PR	SD	PD	NE	%CR	ORR
Arm C	Eligible	32	19 21 30	2	9	1	0	1	66% (47–81%)	94% (79–99%)
	Enrolled	34	21 23 33	2	10	1	0	0	68% (50–83%)	97% (85–100%)
Arm S	Eligible	34	22 23 33	1	10	0	0	1	68% (50–83%)	97% (85–100%)
	Enrolled	35	21 23 33	1	10	0	0	2	66% (44–81%)	94% (81–99%)

Response to each therapy was evaluated according to the International Workshop Criteria for Non-Hodgkin's Lymphoma. CI, confidence interval; CR, complete response; CRu, complete response/unconfirmed; NE, not evaluative due to insufficient follow-up; ORR, overall response rate; PD, progressive disease; PR, partial response; SD, stable disease.

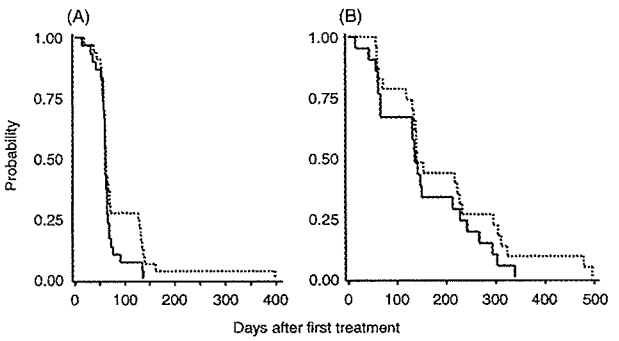

Fig. 1. (A) Time to response (TTR) and (B) time to complete response (TTCR). Medians were estimated by the Kaplan-Meier method. A total of 63 patients (Arm C [-], 30; Arm S [---], 33) were analyzed for TTR, and 44 patients (Arm C, 21; Arm S, 23) for TTCR with per protocol sets of data. Median TTRs in Arm C and Arm S were 61 days (95% confidence interval [CI] 59 to 65 days) and 62 days (95% CI 60–70 days), respectively. The 75th percentile TTRs in Arm C and Arm S were 66 days (95% CI 63 to 76 days) and 140 days (95% CI 66–135 days), respectively ($P = 0.0994$, log–rank test). Median TTCRs in Arm C and Arm S were 136 days (95% CI 65 to 213 days) and 140 days (95% CI 134–227 days), respectively. The 75th percentile TTCRs in Arm C and Arm S were 228 days (95% CI 141 to 293 days) and 295 days (95% CI 153–323 days), respectively ($P = 0.2201$, log–rank test).

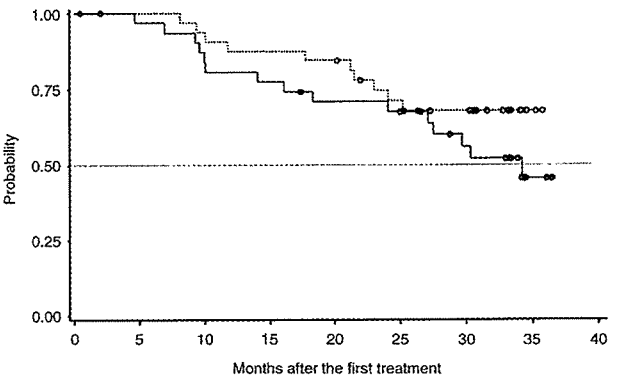

Fig. 2. Progression-free survival (PFS). Medians were estimated by the Kaplan-Meier method. The upper limit of the 95% confidence interval (CI) for Arm C has not yet been determined. A total of 65 patients (Arm C, 32; Arm S, 33) were analyzed with per protocol sets of data. The median PFS time for patients in Arm C (-) was 34.2 months (95%CI, 27.1 months, inestimable), whereas that for patients in Arm S (...) had not yet been reached, with a median follow-up time of 28.2 months. Log–rank test, $P = 0.220$. (o) Censored.

to belong to the low, or low-intermediate risk group categorized by FLIPI. Three patients were judged ineligible by an extramural review committee, because two of them had concomitant active cancer and one had a history of prior chemotherapy, including doxorubicin for the treatment of breast cancer. Sixty-five patients (94%) were confirmed to have FL in the central pathology review.

Response to treatment and survival

Sixty-six eligible patients (Arm C, 32 patients; Arm S, 34 patients) were evaluated with PPSs of data, and 69 patients (Arm C, 34 patients; Arm S, 35 patients) with FASs of data. One patient allocated to Arm C could not be evaluated for response because the first cycle of chemotherapy given was not CHOP (doxorubicin in the CHOP regimen was erroneously replaced with daunorubicin). Two patients (one patient eligible and one ineligible) allocated to Arm S could not be evaluated because they had withdrawn from the study before starting treatment.

As shown in Table 2, similar results of the ORRs and the percentage CRs were obtained in Arm C and Arm S. The ORRs and percentage CRs calculated with PPSs and FASs were similar. Kaplan-Meier curves of TTR and TTCR were plotted for eligible and evaluative patients in each arm, as shown in Fig. 1. Although the median TTRs for patients in Arm C and Arm S were not different (61 days *versus* 62 days, respectively), the 75th percentile TTRs for patients were shorter in Arm C (66 days) than Arm S (127 days), with no statistical difference ($P = 0.0994$, log–rank test). The median TTCRs were similar in Arm C and Arm S (136 days and 140 days, respectively). As shown in Fig. 2, the median PFS time for patients in Arm C ($n = 32$) was 34.2 months

doi: 10.1111/j.1349-7006.2006.00173.x
© 2006 Japanese Cancer Association

Table 3. Hematological toxicity

Toxicity	Arm	*n*	Grade 0–2	Grade 3	Grade 4
Any hematological toxicity	Arm C	34	2 (6%)	3 (9%) 32 (94%)	29 (85%)
	Arm S	33	0 (0%)	10 (30%) 33 (100%)	23 (70%)
Leukopenia	Arm C	34	5 (15%)	16 (47%) 29 (85%)	13 (38%)
	Arm S	33	3 (9%)	23 (70%) 30 (91%)	7 (21%)
Neutropenia	Arm C	34	2 (6%)	3 (9%) 32 (94%)	29 (85%)
	Arm S	33	1 (3%)	9 (27%) 32 (97%)	23 (70%)
Thrombocytopenia	Arm C	34	32 (94%)	1 (3%) 2 (6%)	1 (3%)
	Arm S	33	33 (100%)	0 (0%) 0 (0%)	0 (0%)
Anemia	Arm C	34	31 (91%)	3 (9%)	–
	Arm S	33	31 (94%)	2 (6%)	–

Hematological toxicity was evaluated according to the JCOG Toxicity Criteria, an expanded version of the NCI-CTC version 1.0. All hematological toxicities (possibly related to rituximab, or unknown relationship to rituximab) observed during the treatment and follow-up period (for 6 months after the last cycle of CHOP for Arm C, and for 4 months after the last rituximab infusion for Arm S) are listed.

(95%CI, 27.1 months – inestimable), whereas that for patients in Arm S ($n = 33$) had not yet been reached, with a median follow-up time of 28.2 months. One patient (#38) in Arm S died of tumor progression 730 days after the first treatment. No other patients died within approximately 3 years of observation.

Adverse events

Information about AEs was available for 67 patients (Arm C, 34 patients; Arm S, 33 patients) who received protocol treatment. Hematological toxicity was documented at its highest grade throughout the study period. As shown in Table 3, major hematological toxicity was neutropenia; grade 3 or greater neutropenia was observed in 32 patients (94%) in Arm C and in 33 patients (100%) in Arm S; grade 4 neutropenia was seen in 29 patients (85%) in Arm C and in 23 patients (70%) in Arm S. All hematological toxicities were controllable and reversible, although some patients required hematopoietic cytokines.

Grade 3 or greater non-hematological AEs observed during treatment and initial follow-up periods are listed in Table 4. A total of 11 patients (Arm C, seven patients, 21%; Arm S, four patients, 12%) developed 14 events of grade 3 or greater non-hematological adverse events. All non-hematological toxicities were reversible. There was no therapy-related death.

Prognostic factors

Pretreatment factors affecting ORR and PFS were analyzed. Because the sample size of each arm was small, analyses were not performed separately for the two arms, but results were pooled ($n = 64$). There were two factors affecting ORR when analyzed by the Wilcoxon's rank sum test. Patients with PS 0 (41CR, 13PR, 1NC, 0 PD) demonstrated a superior response to those with PS 1 (3CR, 6PR, 0NC, 0PD) ($P = 0.0182$, Wilcoxon's rank-sum). Patients with a tumor size <5 cm (32CR, 6PR, 1NC, 0 PD) had a superior response to those with tumors equal to 5 cm (12CR, 13PR, 0NC, 0 PD) ($P = 0.0066$, Wilcoxon's rank-sum).

However, no factor significantly affected PFS. Multivariate analyses were also performed using the same factors, excluding IPI. There was no factor that independently affected ORR and PFS.

HACA and pharmacokinetics of rituximab

Out of 67 patients who received rituximab, HACA assays were performed for 65 patients (Arm C, 33; Arm S, 32) at 8 months after treatment, and for 64 patients (Arm C, 33; Arm S, 31) at 10 months after treatment. No patient developed HACA. For all 27 patients (Arm C, 14; Arm S 13) who received four rituximab infusions and whose planned monitoring of

Table 4. Grade 3 or greater-non-hematological adverse events

Arm	Patient	Serious adverse event†	Grade‡	Onset timing	Relating drug (causative)
Arm C	#04	Hyperglycemia	3	6th cycle (day 4)	CHOP (diabetes)
($n = 32$)	#07	Hyperglycemia	3	4th cycle (day 2)	CHOP, rituximab
	#13	Hypertension	3	1st cycle (day 3)	CHOP, rituximab
	#21	Total bilirubin elevation	3	2nd cycle (day 5)	– (constitutional)
	#23	Abdominal pain	3	1st cycle (day 9)	CHOP, rituximab
	#58	Acute cholangitis with elevated AST and ALT	3	3rd cycle (day 10)	CHOP, rituximab
	#59	Hyperglycemia, hypertension	3	5th cycle (day 6)	CHOP, rituximab
Arm S	#25	Total bilirubin elevation	3	6th cycle (day 132)	– (constitutional)
($n = 33$)	#56	Diarrhea	4	1st cycle (day 13)	– (alimentary)
		Febrile neutropenia	3	3rd cycle (day 12)	CHOP
		Interstitial pneumonia	3	3rd cycle (day 15)	CHOP
	#62	Total bilirubin elevation	3	4th cycle (day 7)	CHOP
	#69	AST and ALT elevation	3	1st cycle (day 10)	CHOP
				2nd cycle (day 8)	CHOP
				6th cycle (day 29)	CHOP

†Grade 3 or greater adverse events other than hematological toxicities that were observed during the treatment and follow-up period (for 6 months after the last cycle of CHOP for Arm C, and for 4 months after the last rituximab infusion for Arm S). ‡JCOG Toxicity Criteria, an expanded version of the NCI-CTC, version 1.0.

© 2006 Japanese Cancer Association

Table 5. Pharmacokinetic parameters of rituximab

Arm		Dose (mg/day)	AUC (μg. h/mL)	Cmax† (μg/mL)	$T_{1/2}$ (h)	Clearance‡ (litter/h)	MRT (h)	Vd (litter)
Arm C	Mean	593.9	372 498.9	262.5	232.3	0.0259	335.1	4.49
(n = 14)	SD	51.1	111 660.4	73.2	113.8	0.0301	164.2	0.66
Arm S	Mean	596.4	418 901.3	433.5	356.9	0.0128	514.9	5.57
(n = 13)	SD	82.6	107 002.6	134.9	163.4	0.0077	235.9	1.95

†Actual measured value. ‡Calculated under the one-compartment model. Time points for serum collection were as follows; Arm C: before, and 10 min and 2 days after each rituximab infusion, and 1 week, 1, 4 and 6 months after the sixth rituximab infusion. Arm S: before, 10 min after each rituximab infusion and 2 days, 1 and 2 weeks, and 1 and 4 months after the sixth rituximab infusion. AUC, area under the curve; Cmax, maximum concentration; $T_{1/2}$, elimination half-life; MRT, mean residence time; Vd, volume of distribution.

serum rituximab levels were completed, pharmacokinetic parameters were calculated throughout the four infusions. As shown in Table 5, Arm S showed higher values for the parameters of area under the curve (AUC), maximum concentration (Cmax), elimination half-life (T1/2), mean residence time (MRT), and volume of distribution (Vd).

Discussion

In this randomized phase II trial, we have demonstrated that the combined use of rituximab and CHOP yielded an ORR of 94% and 97%, and a percentage CR of 66% and 68% in the concurrent arm and the sequential arm, respectively. These ORRs and percentage CRs are superior to those reported for combination chemotherapy regimens containing anthracycline without rituximab, which were conducted after stringent clinical staging with CT. The percentage CR obtained by six to eight cycles of CHOP chemotherapy in untreated patients (n = 83) with FL was reported to be 36% (90%CI, 27–46%).[30] The ORR and percentage CR of CHOP chemotherapy obtained by Kimby *et al.* in their randomized study comparing chlorambucil plus prednisone *versus* CHOP in symptomatic low-grade NHL (n = 127), were 60% and 18%, respectively.[31]

Data of the present study was comparable to the preceding study on CHOP combined with rituximab in patients with indolent B-NHL regarding efficacy and tolerability. Although the precise schedule of the administration of rituximab in the first phase II study of R-CHOP reported by Czuczman *et al.* was not the same as that of the present study, the concept of concurrent use is identical between their trial and Arm C in the present study.[14] However, the percentage CR of Arm C is less than that of Czuczman *et al.*'s trial, and the median PFS of Arm C appears to be shorter in the present study, although more than 82% of all enrolled patients in our study were in the low or low-intermediate risk group by FLIPI. In Czuczman *et al.*'s trial, as the last two infusions of rituximab were administered 1 month after the sixth CHOP cycle, like in our sequential arm, the design of Czuczman *et al.*'s trial had characteristics of both the concurrent arm and the sequential arm. So it is possible that the higher percentage CR and longer PFS in Czuczman *et al.*'s trial compared to our concurrent arm were partly due to the mixed design of the administration schedule of rituximab, in addition to the possible selection bias in phase II studies.

The South-west Oncology Group (SWOG) in the USA studied six cycles of CHOP followed by four weekly infusions of rituximab in newly diagnosed patients with FL at advanced stages (31% with bulky disease and 30% with B-symptoms). Sixteen (19%) of the 84 evaluative patients had an improved tumor response after rituximab treatment, with an ORR of 72%, including 54% with a CR or CRu. The PFS was 76% at the median follow-up of 2.7 years.[32] The PFS data of the sequential arm in our trial is similar to that of the SWOG trial.

Cancer and Leukemia Group B (CALGB) conducted a randomized phase II study to explore a more suitable administration schedule of rituximab with fludarabine in previously untreated chronic lymphocytic leukemia (CLL) patients.[33] Patients randomly received either six monthly courses of fludarabine concurrently with rituximab followed 2 months later by four weekly doses of rituximab for consolidation therapy, or fludarabine alone followed 2 months later by rituximab consolidation therapy. The ORR with the concurrent regimen was 90% compared to 77% with the sequential regimen. With a median follow-up time of 23 months, the number of relapsed patients was 18 (35%) in the concurrent regimen and 15 (28%) in the sequential regimen. Although PFS and survival appeared to be somewhat longer with the sequential treatment, CALGB concluded that the concurrent use of rituximab and fludarabine was superior. Our randomized phase II study for indolent B-cell NHLs showed similar percentage ORRs and percentage CRs between the two arms, and a seemingly longer PFS in the sequential arm. Because patients in the concurrent arm in the CALGB study received consolidated administration of rituximab after induction therapy, the concurrent arm in the CALGB study had characteristics of the concurrent arm and sequential arm of our present study.

In a randomized phase III study that compared eight cycles of R-CVP to CVP for previously untreated patients with advanced FL, a significantly prolonged TTP of R-CVP was reported (median 32 months *versus* 15 months for CVP; $P < 0.0001$).[18] The median TTP of R-CVP was similar to the median PFS of Arm C in our study. As the toxicity is stronger in CHOP than CVP, it is worthwhile to conduct a randomized phase III trial to compare R-CHOP to R-CVP.

The maintenance use of rituximab after first-line rituximab therapy was also reported to prolong PFS or event-free survival (EFS).[34,35] Future trials to explore the role of maintenance use of rituximab after first-line rituximab containing chemotherapy like Arm C are warranted.

About 25% of patients in Arm S did not achieve a response (PR or higher) before the initiation of rituximab treatment, despite the completion of six cycles of CHOP. In Arm C, more than 90% of patients showed a response after the six cycles of CHOP plus rituximab. The same tendency was also shown in the TTCR, as shown in Fig. 1B. The TTCR of each patient in Arm C was relatively shorter than that in Arm S.

doi: 10.1111/j.1349-7006.2006.00173.x
© 2006 Japanese Cancer Association

While grade 3 or greater non-hematological AEs were observed in 11 patients (Arm C, seven patients, 21%; Arm S, four patients, 13%), both arms were well tolerated. Two patients were withdrawn from the study before completion of the planned treatment by AE. One patient in Arm C developed acute cholangitis after the third cycle of CHOP plus rituximab. The other patient in Arm S developed interstitial pneumonia after the third cycle of CHOP. Both patients fully recovered. Hematological toxicities were observed in all treated patients; grade 4 neutropenia was frequent and was observed in 85% of patients in Arm C and in 70% in Arm S. However, these hematological toxicities were manageable with or without supportive care using hematopoietic growth factor. No patient was withdrawn from the study due to hematological toxicity. Grade 3 or greater thrombocytopenia was rare in Arm C and absent in Arm S. Although hematological and non-hematological toxicities were slightly more frequent in Arm C, toxicities were clinically acceptable in both arms.

In conclusion, CHOP combined with rituximab was highly effective in untreated patients with indolent B-NHL, especially FL, either in a concurrent or sequential combination, with acceptable toxicities. Although the time to achieve a response was more rapid with the concurrent combination than the sequential combination, PFS appeared to be slightly longer with the sequential combination, although the difference was not statistically significant. We conclude that both combination schedules deserve further investigation. Considering the promising results of rituximab maintenance therapy reported by other investigators, it would be worthwhile to conduct future trials to establish the role of rituximab maintenance after concurrent and sequential combinations of rituximab plus CHOP therapy.

Acknowledgments

This study was supported by Zenyaku Kogyo, Tokyo, Japan. We thank all the investigators, including the physicians, nurses and laboratory technicians, in the participating institutions of this multicenter trial. We are grateful to Dr K. Oshimi (Juntendo University School of Medicine, Tokyo), Dr K. Toyama (Tokyo Medical College, Tokyo), and Dr S. Shirakawa (Koudoukai Hospital, Osaka) for their critical review of the clinical data as members of the Independent Monitoring Committee. We are grateful to Dr S. Nakamura (Aichi Cancer Center Hospital, Nagoya), Dr Y. Matsuno (National Cancer Center Hospital, Tokyo), Dr S. Nawano (National Cancer Center Hospital East, Kashiwa), and Dr M. Matsusako (St. Luke's International Hospital, Tokyo) for their central pathological or radiographical review as members of the Central Pathological Review Committee and the Central Response-Evaluating Committee. We also acknowledge Y. Arita, K. Endo, T. Uesugi, M. Tachikawa, Y. Ikematsu, T. Itoh, H. Iimura, K. Inatomi, M. Ikenami, Y. Koide and T. Kayo (Zenyaku Kogyo) for their help with data collection and statistical and pharmacological analyses.

References

1 Rohatiner A, Lister TA. *Follicular lymphoma, in Magrath IT (ed.): The Non-Hodgkin's Lymphomas*. London: Oxford University Press, 1997: 867–96.
2 Berger F, Felman P, Sonet A *et al.* Nonfollicular small B-cell lymphomas: a heterogeneous group of patients with distinct clinical features and outcome. *Blood* 1994; **83**: 2829–35.
3 Horning SJ. Natural history of and therapy for the indolent non-Hodgkin's lymphomas. *Semin Oncol* 1993; **20**: 75–88.
4 Solal-Celigny PH. Management of histologically indolent non-Hodgkin's lymphomas. *Baillieres Clin Hematol* 1996; **9**: 669–87.
5 Aisenberg AC. Coherent view of non-Hodgkin's lymphoma [review]. *Clin Oncol* 1995; **13**: 2656–75.
6 Reff M, Carner K, Chambers K *et al.* Depletion of B cells in vivo by a chimeric mouse human monoclonal antibody to CD20. *Blood* 1994; **83**: 435–45.
7 Taji H, Kagami Y, Okada Y *et al.* Inhibition of CD20-positive B lymphoma cell lines by IDEC-C2B8 anti-CD20 monoclonal antibody. *Jpn J Cancer Res* 1998; **89**: 748–56.
8 Demidem A, Lam T, Alas S, Hariharan K, Hanna N, Bonavida B. Chimeric anti-CD20 (IDEC-C2B8) monoclonal antibody sensitizes a B cell lymphoma cell line to cell killing by cytotoxic drugs. *Cancer Biother Radiopharm* 1997; **12**: 177–86.
9 McLaughlin P, Grillo-Lopez AJ, Link BK *et al.* Rituximab chimeric anti-CD20 monoclonal antibody therapy for relapsed indolent lymphoma: Half of patients respond to a four-dose treatment program. *J Clin Oncol* 1998; **16**: 2825–33.
10 Foran JM, Gupta RK, Cunningham D *et al.* A UK multicentre phase II study of rituximab (chimaeric anti-CD20 monoclonal antibody) in patients with follicular lymphoma, with PCR monitoring of molecular response. *Br J Haematol* 2000; **109**: 81–8.
11 Hainsworth JD, Burrism HA, Morrissey LH *et al.* Rituximab monoclonal antibody as initial systemic therapy for patients with low grade non-Hodgkin's lymphoma. *Blood* 2000; **95**: 3052–6.
12 Colombat P, Salles G, Brousse N *et al.* Rituximab (anti-CD20 monoclonal antibody) as single first-line therapy for patients with follicular lymphoma with a low tumor burden: Clinical and molecular evaluation. *Blood* 2001; **97**: 101–6.
13 Igarashi T, Kobayashi Y, Ogura M *et al.* Factors affecting toxicity, response and progression-free survival in relapsed patients with indolent B-cell lymphoma and mantle cell lymphoma treated with rituximab: a Japanese phase II study. *Ann Oncol* 2002; **13**: 928–43.
14 Czuczman MS, Grillo-Lopez AJ, White CA *et al.* Treatment of patients with low-grade B-cell lymphoma with the combination of chimeric anti-CD20 monoclonal antibody and CHOP chemotherapy. *J Clin Oncol* 1999; **17**: 268–76.
15 Czuczman MS, Weaver R, Alkuzweny B, Berlfein J, Grillo-Lopez AJ. Prolonged clinical and molecular remission in patients with low-grade or follicular non-Hodgkin's lymphoma treated with rituximab plus CHOP chemotherapy: 9-year follow-up. *J Clin Oncol* 2004; **22**: 4711–6.
16 Forstpointner R, Dreyling M, Repp R *et al.* The addition of rituximab to a combination of fludarabine, cyclophosphamide, mitoxantrone (FCM) significantly increases the response rate and prolongs survival as compared with FCM alone in patients with relapsed and refractory follicular and mantle cell lymphomas: results of a prospective randomized study of the German Low-Grade Lymphoma Study Group. *Blood* 2004; **104**: 3064–71.
17 Czuczman MS, Koryzna A, Mohr A *et al.* Rituximab in combination with fludarabine chemotherapy in low-grade or follicular lymphoma. *J Clin Oncol* 2005; **23**: 694–704.
18 Marcus R, Imrie K, Belch A *et al.* CVP chemotherapy plus rituximab compared with CVP as first-line treatment for advanced follicular lymphoma. *Blood* 2005; **105**: 1417–23.
19 Harris NL, Jaffe ES, Stein H *et al.* A revised European-American classification of lymphoid neoplasms: a proposal from the International Lymphoma Study Group. *Blood* 1994; **84**: 1361–92.
20 Carbone PP, Kaplan HS, Musshoff K, Smithers DW, Tubiana M. Report of the committee on Hodgkin's disease staging classification. *Cancer Res* 1971; **31**: 1860–1.
21 Oken MM, Creech RH, Tormey DC *et al.* Toxicity and response criteria of Eastern Cooperative Oncology Group. *Am J Clin Oncol* 1982; **5**: 649–55.

© 2006 Japanese Cancer Association